Published by Institute of Physics Publishing for SISSA/ISAS
Received: *May 1, 2002*
Revised: *June 10, 2002*
Accepted: *June 12, 2002*

Photon and gluon emission in relativistic plasmas

Peter Arnold

Department of Physics, University of Virginia
Charlottesville, Virginia 22901, USA
E-mail: parnold@virginia.edu

Guy D. Moore and Laurence G. Yaffe

Department of Physics, University of Washington
Seattle, Washington 98195, USA
E-mail: guymoore@phys.washington.edu, yaffe@phys.washington.edu

Abstract: We recently derived, using diagrammatic methods, the leading-order hard photon emission rate in ultra-relativistic plasmas. This requires a correct treatment of multiple scattering effects which limit the coherence length of emitted radiation (the Landau-Pomeranchuk-Migdal effect). In this paper, we provide a more physical derivation of this result, and extend the treatment to the case of gluon radiation.

Keywords: Thermal Field Theory, Electromagnetic Processes and Properties, QCD.

http://jhep.sissa.it/archive/papers/jhep062002030/jhep062002030.pdf

Contents

JHEP06(2002)030

1. Introduction

The rate of photon emission in a high-temperature QCD plasma is a problem of some theoretical interest [1]–[14], due in part to the hope that hard photon emission will be a useful diagnostic probe of heavy ion collisions [15, 16]. Understanding the analogous rate of gluon emission in a hot QCD plasma is required for computing thermalization and transport processes [17]–[24].

We will make the simplifying assumption that the temperature T is so large that the running strong coupling constant $g_{\rm s}(T)$ can be treated as small, and focus on the leading-order (in $\alpha_{\rm s}$) behavior of the photon or gluon emission rate.[1] Evaluating just the leading weak coupling behavior, even in this asymptotically high temperature regime, is non-trivial. For the photon emission rate, one might expect that it would be sufficient to compute just the diagrams shown in figure 1, which describe lowest order two-to-two particle scattering processes. But it turns out that naive perturbation theory (augmented by the standard resummation of hard thermal loops) does not suffice to calculate the leading-order hard photon emission rate. Figure 2 shows bremsstrahlung and pair annihilation processes which also contribute to the on-shell photon emission rate at leading order. The essential problem

[1]In other words, we will neglect all sub-leading corrections to the emission rate suppressed by additional powers of $\alpha_{\rm s}$, as well as power corrections suppressed by $\Lambda_{\rm QCD}/T$ or m_q/T.

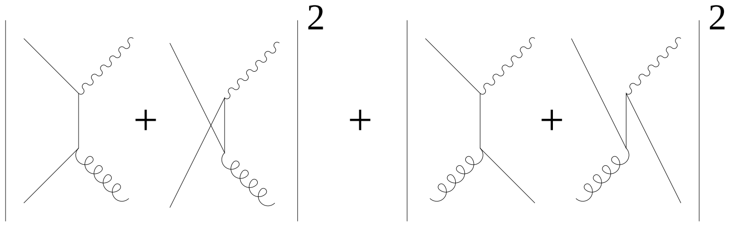

Figure 1: Two-to-two particle processes contributing to the leading order photon emission rate. Time may be viewed as running from left to right.

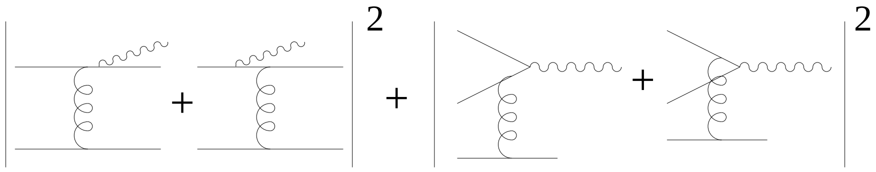

Figure 2: Bremsstrahlung and pair annihilation contributions to photon emission. The bottom line in each diagram can represent either a quark or a gluon.

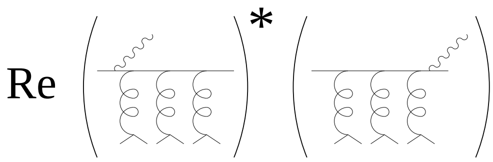

Figure 3: An interference term, involving amplitudes for photon emission before and after multiple scattering events, which contributes to the leading order emission rate.

is that the internal time scale associated with these processes is comparable to the mean free time for soft scattering with other particles in the plasma. Consequently, even at leading order, the photon emission rate is sensitive to processes involving multiple scatterings occurring during the emission process. This is known as the Landau-Pomeranchuk-Migdal (LPM) effect. Diagrammatically, it manifests as the presence of interference terms involving multiple collisions, such as depicted in figure 3, which parametrically are equally as important as those of figure 2. In the nearly-collinear limit, the extra explicit factors of $g_{\rm s}$ turn out to be canceled by a combination of parametrically large enhancements from the internal quark propagators and soft exchanged gluons.

In ref. [25], we showed how to account for the LPM effect in photon emission by identifying and summing the appropriate infinite class of diagrams which contribute to the leading order emission rate, and in ref. [26] we solved the resulting integral equations numerically. Our analysis in ref. [25] involved quite detailed power counting of diagrams and relied upon some rather unintuitive relationships found by Wang and Heinz [27] between real-time thermal 4-point Green's functions in the r/a (Keldysh) formalism. One goal of the present article is to reproduce our previous results in a manner that more clearly highlights the essential physics of the result. We will embrace physical arguments wherever possible, leaving to our previous work [25] the more technical justification of our results. Our second goal will be to extend the treatment to the case of gluon emission.

We are hardly the first people to discuss applications of the LPM effect, either qualitatively or quantitatively [13], [18]–[24], [28]–[33].[2] However, discussions prior to our work [25] have almost always focused on systems where the scatterers with which the emitting particle interacts are static. (The scatterers are represented by the bottom lines in figures 2 and 3.) But typical scatterings in an ultra-relativistic plasma involve interactions with excitations which are themselves moving at nearly the speed of light. They produce dynamically screened color electric and magnetic fields which form a fluctuating background field in which bremsstrahlung, pair annihilation, and the LPM effect take place.

Our discussion will be largely self-contained and will not directly rely on previous treatments of the LPM effect in other contexts. One could, presumably, explicitly mimic previous discussions such as the seminal 1955 analysis of Migdal [29, 30], and suitably generalize the treatment to non-static scattering. However, it is rather challenging to follow in detail all of the assumptions and approximations made in Migdal's quantum mechanical treatment. We believe that readers interested in understanding the effect can benefit from several different formulations. Moreover, our discussion of scales and approximations will be tailored to the particular problem at hand, namely hard photon (and later gluon) emission in ultra-relativistic plasmas.

We will focus on the contributions of bremsstrahlung and pair annihilation to the rate of photon (or gluon) emission. We will not explicitly discuss contributions to the emission rate from the $2 \leftrightarrow 2$ processes of figure 1, which are of the same order but do not require a treatment of the LPM effect. These $2 \leftrightarrow 2$ contributions to the photon emission rate are calculated in ref. [9, 10, 26].[3] Diagrammatically, the bremsstrahlung and pair annihilation processes of figure 2 look like they are suppressed by an explicit factor of $g_{\rm s}^2$ compared to the $2 \leftrightarrow 2$ processes of figure 1. However, the diagrams of figure 2 have a collinear enhancement, associated with emission of the photon. This enhancement is produced by a would-be collinear singularity which is cut off by the effective thermal mass (of order $g_{\rm s}T$) and width of the fermions, yielding a parametrically large near on-shell enhancement which causes these processes to be the same order (up to a logarithm of $g_{\rm s}$) as those of figure 1.

We will use the following nomenclature in our discussion. The particles corresponding to the lower lines in figures 2 or 3 will be called the scatterers. The particle which emits the photon in bremsstrahlung, or the particle/anti-particle pair which annihilate in pair annihilation, will be called the (photon) emitters. Each separate gluon exchange in figures 2 and 3 will be referred to as a "scattering" of the emitters.[4]

[2] For a review of many aspects of the LPM effect, with an emphasis on the theory and experiment of high-energy collisions of electrons with atomic matter, see ref. [34].

[3] Only the $k \gg T$ limit is addressed in refs. [9, 10].

[4] When distinguishing emitters from scatterers, one need not worry about the fundamental indistinguishability of quarks in, say, quark-quark scattering, because the scattering is dominated by small angle collisions, and the photon is emitted nearly collinear with the emitter(s). So, at leading order, emitters and scatterers are distinguishable simply by whether or not their direction of motion is nearly aligned with the emitted photon.

JHEP06(2002)030

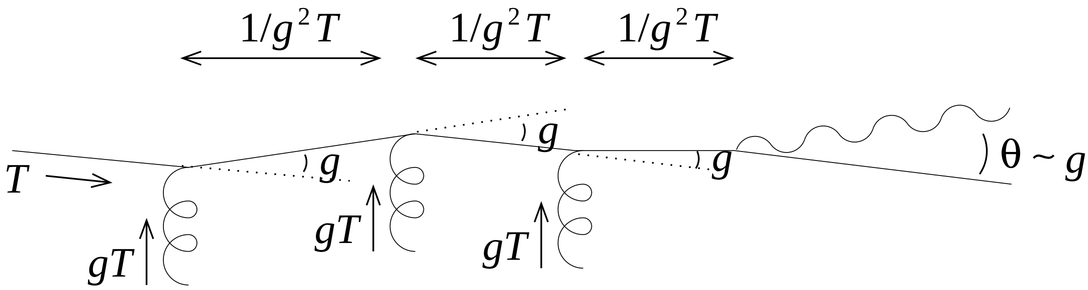

Figure 4: Orders of magnitude of various momentum, distance, and angular scales associated with bremsstrahlung of a photon with momentum of order T. g stands for the strong coupling $g_{\rm s}$.

Before we begin, we first summarize the basic scales associated with bremsstrahlung and pair annihilation of hard photons via the processes of figure 2. For simplicity, we restrict attention to photons with momenta parametrically of order T, which is the typical momentum of particles in the ultra-relativistic plasma. We will throughout treat electromagnetic couplings as small compared to the QCD coupling, and we will ignore thermal effects on the propagation of the photon (which are proportional to $\alpha_{\rm EM}$). The basic kinematics, summarized pictorially in figure 4 for bremsstrahlung, turn out to be as follows.

- The typical momenta of the emitters and scatterers is order T.
- The typical momentum transfer q of an exchanged gluon responsible for scattering during the emission of the photon is of order $g_{\rm s}T$, which is also the order of the inverse Debye screening length for color. The angle of deflection in such a collision is of order this momentum transfer divided by the emitter momentum of order T, hence $\theta \sim g_{\rm s}$.
- Processes contributing to the leading-order emission rate are dominated by nearly collinear emission of the photon. The corresponding internal quark lines in figure 2 are nearly on-shell, with energies off-shell by an amount δE of order $g_{\rm s}^2 T$. Fourier transforming, this implies that these processes have time durations of order $(g_{\rm s}^2 T)^{-1}$. This is known as the *formation time* of the photon.
- The formation time scale $(g_{\rm s}^2 T)^{-1}$ is also the order of the mean free time between collisions with momentum transfers of order $g_{\rm s}T$. This is why multiple collisions cannot be treated independently and interferences such as figure 3 must be included at leading order.
- The typical angle between the directions of the photon and the emitter(s) (be they initial state or final state emitters) is $\theta \sim g_{\rm s}$.
- The typical angle between the directions of the emitter and a scatterer is $O(1)$.

A brief review of how to obtain these scales is given in section I.B of ref. [25]. Here, we will take them as our starting point and proceed to discuss how to sum up the effects of multiple collisions.

JHEP06(2002)030

Certain physical processes in high temperature gauge theories (such as the rate of baryon number violation in hot electroweak theory) are sensitive to "ultra-soft" collisions which are mediated by low-frequency non-abelian magnetic fluctuations with momentum transfers of order $g_s^2 T$. The dynamics of such ultra-soft collisions are intrinsically non-perturbative. One may check *a posteriori*, by inspection of the final answers we will produce, that the leading-order dynamics relevant for hard photon (or gluon) production is not sensitive to ultra-soft collisions. Alternatively, the reader may find detailed qualitative and diagrammatic discussions of this point in ref. [25].

For simplicity, we will restrict attention to the case of zero chemical potential. The generalization of results for photon emission to non-zero chemical potential may be found in ref. [25]. In the next section, we will mainly focus on bremsstrahlung and reformulate the problem as that of bremsstrahlung from an emitter that is propagating through a classical random background color gauge field. We will show how simple physical considerations of localization of particles in both space and momentum lead to a description of the LPM effect in bremsstrahlung as an infinite sum of ladder diagrams. In section 3, we will discuss how to convert the required sum of ladder diagrams into a Boltzmann-like integral equation—a task previously carried out in ref. [25], but which we will repeat using the formalism of this paper, in a way that more clearly displays which portions of the relevant physics depend on the nature of the emitter (e.g. an actual Dirac quark, a fictitious scalar quark, or something else) and which physics does not. In section 4, we then analyze the closely related process of pair annihilation, and we combine these results for photon emission in section 5. Finally, in section 6 we discuss the generalization to gluon emission.

2. Random backgrounds and ordering of interactions

The differential photon emission rate (per unit volume), at leading order in $\alpha_{\rm EM}$, is given by the well-known relation

$$d\Gamma_\gamma = \frac{d^3\mathbf{k}}{(2\pi)^3\, 2|\mathbf{k}|} \sum_{a=1,2} \epsilon^\mu_{(a)}(\mathbf{k})^* \, \epsilon^\nu_{(a)}(\mathbf{k})\, W_{\mu\nu}(K)\,, \tag{2.1}$$

where $K = (k^0, \mathbf{k}) = (|\mathbf{k}|, \mathbf{k})$ denotes the null photon 4-momentum, the ϵ's represent a basis of transverse polarizations for the photon, and $W_{\mu\nu}(K)$ is the Wightman electromagnetic current-current correlator,

$$W_{\mu\nu}(K) = \int d^4x\, e^{-iKx}\, \langle j_\mu(0) j_\nu(x)\rangle\,. \tag{2.2}$$

We use a metric with signature $(-{+}{+}{+})$. Because the correlator is contracted with photon polarization vectors in (2.1), one need only consider the case where μ and ν are spatial indices in what follows. As always, $\langle\cdots\rangle$ denotes an expectation value in whatever density matrix $\mathcal{P}$ is of interest, which in our case is a thermal ensemble describing the equilibrium plasma. If one inserts a complete set of multi-particle states $|f\rangle$ between the currents, and works in a basis $|i\rangle$ where $\mathcal{P}$ is diagonal, then the correlator $W_{\mu\nu}$ can also be written as

$$W_{\mu\nu}(K) = \int d^4x\, e^{-iKx} \sum_{i,f} \mathcal{P}_i\, \langle i|j_\mu(0)|f\rangle\, \langle f|j_\nu(x)|i\rangle\,. \tag{2.3}$$

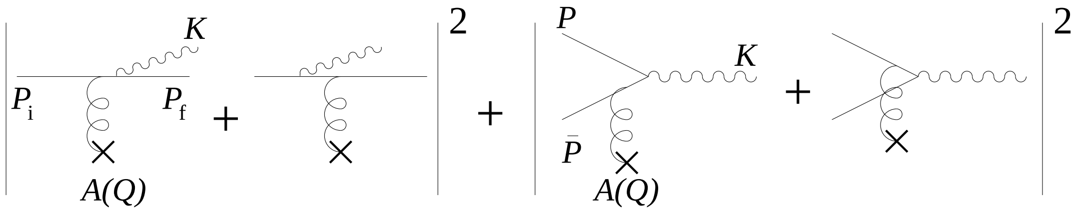

Figure 5: The perturbative bremsstrahlung and annihilation processes of figure 2, with the soft gluon fields now interpreted as classical background fields.

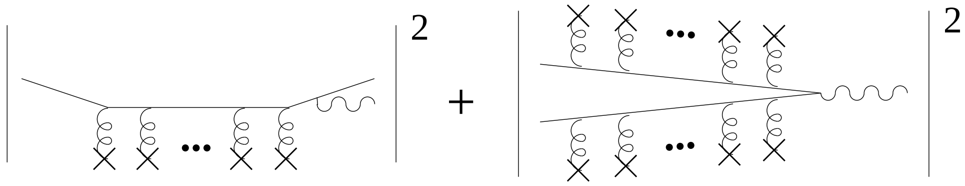

Figure 6: Bremsstrahlung and annihilation processes including the multiple interactions with a background field, which lead to the LPM effect.

It will be useful to remember that this corresponds to scattering from an initial state i to a final state f plus the emitted photon. Moreover, the integrand in (2.3) can be interpreted as representing interference between photon emission at the space-time points 0 and x.

Our first approximation will be to treat the soft ($q \sim gT$) gluons of the problem as a random, *classical* non-abelian background field $A_\mu(x)$, through which the particles that bremsstrahlung or annihilate propagate. The lowest-order processes of figure 2 are then replaced by figure 5, and our task will be to sum up multiple gluon interactions such as depicted in figure 6. After computing rates, we will appropriately average over this random classical gauge field. Such averaging will be denoted by $\langle\!\langle \cdots \rangle\!\rangle$. By translation invariance, the variance of the background field must have the form[5]

$$\langle\!\langle A^\mu(Q)^* \, A^\nu(Q') \rangle\!\rangle = \rho_A^{\mu\nu}(Q) \; (2\pi)^4 \delta^{(4)}(Q{-}Q') \,, \tag{2.4}$$

where $\rho_A^{\mu\nu}(Q)$ is the spectral density of thermal gauge field fluctuations. We may treat the statistical distribution of the background gauge field as gaussian, dropping higher-order connected correlations. This is equivalent to neglecting the nonlinear self-interaction of the background and neglecting the interactions between different scatterers. This approximation is valid, at leading order, everywhere except in the deep infrared ($Q \sim g^2T$). Neglecting non-gaussian correlations in the background gauge field would not be allowable if the processes under consideration were sensitive (at leading order) to ultra-soft g^2T fluctuations. Fortunately, this is not the case [25].

Physically, these soft gauge fields are created by other charge carriers [with typical $O(T)$ momenta] passing randomly through the plasma. The statistics of the soft gauge fields generated by these particles can be described using (i) the fluctuation-dissipation theorem, and (ii) the standard hard thermal loop (HTL) approximation for the retarded self-energy

[5] A translationally invariant choice of gauge fixing, such as Lorentz or Coulomb gauge, is tacitly assumed.

$\Pi(Q)$ of soft ($Q \ll T$) gauge fields. Namely, the spectral density $\rho_A(Q) \equiv ||\rho_A^{\mu\nu}(Q)||$ may be taken to be

$$\begin{aligned}\rho_A(Q) &\simeq 2[n_{\rm b}(q^0)+1]\,{\rm Im}\,G^{\rm HTL}_{\rm Ret}(Q)\\ &= 2[n_{\rm b}(q^0)+1]\;{\rm Im}\left[\frac{1}{G^{(0)}_{\rm Ret}(Q)^{-1}+\Pi^{\rm HTL}_{\rm Ret}(Q)}\right],\end{aligned} \tag{2.5}$$

where $n_{\rm b}(\omega) = 1/(e^{\beta\omega}-1)$ is the Bose distribution function, $G^{(0)}_{\rm Ret}(Q)$ is the free retarded gauge field propagator, and $G^{\rm HTL}_{\rm Ret}(Q)$ is the retarded propagator with hard thermal loops resummed, which account for Debye screening and Landau damping of the color fields. We will review the specific formulas later, in section 5. Because the background fields of interest are soft, one may replace the $[n_{\rm B}(q^0)+1]$ statistical factor by its low frequency limit, namely T/q^0.

The presence of correlations in the background field with non-trivial frequency (and wave-number) dependence is the most significant difference between our problem of hard photon emission in a relativistic plasma, and the original setting for the LPM effect of hard photon emission in a static medium of random Coulomb scatterers (nuclei). In order to be able to make contact later between our results and those of Migdal, we will treat the spectral density $\rho_A(Q)$ as arbitrary, and not use the specific form (2.5) until the very end.

2.1 Particle propagation in a random field

Our next task is to rewrite the current correlator (2.2) in terms of propagation amplitudes of single particle states in the random background. We will focus on the bremsstrahlung process and come back to pair annihilation in section 4. Bremsstrahlung corresponds to a contribution to the current correlator (2.2) of the form[6]

$$W^{\rm brem}_{\mu\nu}(K) = \int d^4x\, e^{-iKx} \int_{\mathbf{p}_i\mathbf{p}_f} n(p_i)[1\pm n(p_f)] \left\langle\!\!\left\langle \langle \mathbf{p}_i|j_\mu(0)|\mathbf{p}_f\rangle\, \langle \mathbf{p}_f|j_\nu(x)|\mathbf{p}_i\rangle \right\rangle\!\!\right\rangle, \tag{2.6}$$

where $|\mathbf{p}_i\rangle$ and $|\mathbf{p}_f\rangle$ represent one-particle states of the emitting charge carrier, and n is the corresponding equilibrium distribution function [either $n_{\rm b}(p)$ or $n_{\rm f}(p)$]. The contributions (2.6) to the current correlator have to be summed over all types (including anti-particles) and spins of hard charged quasi-particles. The momenta $\mathbf{p}_i$ and $\mathbf{p}_f$ can be regarded as the initial and final momenta of the charge carrier, and $n(p_i)$ and $1 \pm n(p_f)$ are the initial and final state statistical factors. There is an approximation hiding here because momentum eigenstates $|\mathbf{p}\rangle$ are not exact energy eigenstates in the presence of the soft background field. The density matrix is not therefore precisely $n(p)$. Over the $O(1/g^2T)$ formation time relevant to our problem, soft momenta transfers change $\mathbf{p}$ by order $gT \ll p$. But the resulting error in the use of $n(p)$ is then sub-leading in g and so can be ignored in a leading-order analysis.

[6] For any three-momentum $\mathbf{p}$, $\int_{\mathbf{p}}$ means $\int d^3\mathbf{p}/(2\pi)^3$, while for a four-vector Q, $\int_Q$ will denote $\int d^4Q/(2\pi)^4$.

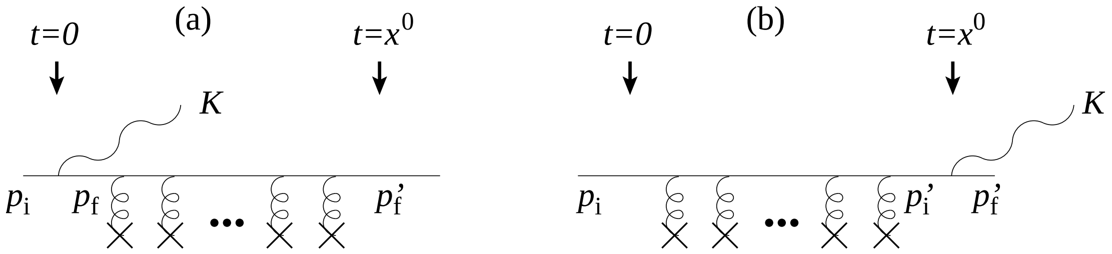

Figure 7: Two diagrams, time ordered from left to right, whose interference contributes to the rate of bremsstrahlung. The first diagram represents photon emission at time zero, and the second at time x^0, and in both cases the diagrams show the evolution between these two times.

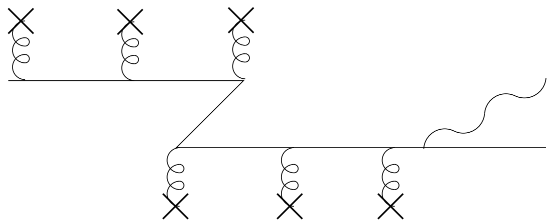

Figure 8: A time-ordered Z diagram.

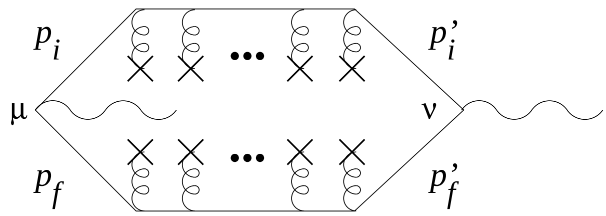

Figure 9: A single diagram depicting the interference of the two diagrams of figure 7. The interactions along top and bottom lines are independently time ordered from left to right.

Making the time evolution explicit, and inserting complete sets of intermediate states, the statistically averaged matrix elements appearing in (2.6) can be rewritten as

$$\int_{\mathbf{p}'_i \mathbf{p}'_f} \left\langle\!\!\left\langle \langle \mathbf{p}_i | j_\mu(0) | \mathbf{p}_f \rangle \, \langle \mathbf{p}_f | U(0, x^0) | \mathbf{p}'_f \rangle \, \langle \mathbf{p}'_f | j_\nu(\mathbf{x}) | \mathbf{p}'_i \rangle \langle \mathbf{p}'_i | U(x^0, 0) | \mathbf{p}_i \rangle \right\rangle\!\!\right\rangle$$
$$= \int_{\mathbf{p}'_i \mathbf{p}'_f} \langle \mathbf{p}_f | j_\mu(0) | \mathbf{p}_i \rangle^* \, \langle \mathbf{p}'_f | j_\nu(\mathbf{x}) | \mathbf{p}'_i \rangle \left\langle\!\!\left\langle \langle \mathbf{p}'_f | U(x^0, 0) | \mathbf{p}_f \rangle^* \, \langle \mathbf{p}'_i | U(x^0, 0) | \mathbf{p}_i \rangle \right\rangle\!\!\right\rangle , \tag{2.7}$$

where $U(t', t)$ is the time evolution operator in the background field. As usual, the spatial Fourier transform in (2.6) combines with translation invariance (of the statistically averaged matrix elements) to enforce total momentum conservation:

$$\mathbf{k} = \mathbf{p}_i - \mathbf{p}_f = \mathbf{p}'_i - \mathbf{p}'_f \, . \tag{2.8}$$

Diagrammatically, this contribution represents the interference in the evolution of the particle from time 0 to x^0 depending on whether the photon is emitted at time 0 or at time x^0, as depicted in figures 7a and b. These diagrams can be considered as time ordered (with time running from left to right) because each individual $Q \sim gT$ momentum transfer is not enough to create or destroy a (nearly on-shell) particle/anti-particle pair. That is, in a time-ordered Z contribution like figure 8, the three-particle intermediate state would have to be so far off shell that its contribution is suppressed compared to the time ordering of figure 7a. It is convenient to put the interference of the evolutions of figures 7 together into the single diagram depicted by figure 9. The top line (or "rail") represents $\langle \mathbf{p}_i' | U(x^0, 0) | \mathbf{p}_i \rangle$ and the bottom line (rail) the complex conjugate of $\langle \mathbf{p}_f' | U(x^0, 0) | \mathbf{p}_f \rangle$. This looks just like a Feynman diagram for the current correlator, except with the added interpretation that each rail of the diagram can be considered as time ordered from left to right.

2.2 Ordering of interactions

The next step is to understand the effect of averaging over the background gauge field. A quick way to visualize the dominant correlations is to think of the photon and emitter qualitatively as approximately classical particles, having both approximately well-defined position and momentum, obeying roughly

$$\mathbf{x}(t) \simeq \mathbf{x}(0) + \mathbf{v_p}\, t\,. \tag{2.9}$$

Indeed, the original, qualitative derivation of the LPM effect was purely classical [28].[7] (See section 1 of ref. [24] for a concise review.) More formally, instead of using a basis of momentum or position states, one may use an (over-complete) basis of gaussian wave packets with width $\Delta x \sim (\Delta p)^{-1} \sim (gT)^{-1}$. For momenta of order T, the widths will remain of this order over the time scale $1/g^2T$ relevant to our problem.[8] The spatial uncertainty Δx in the position of the particles is then always small compared to $1/g^2T$, which is the mean free path for the soft gluon interactions with $Q \sim gT$ which dominate our problem. This implies that interactions with scatterers must occur in a definite order, regardless of when the bremsstrahlung photon is emitted.

Figure 10 illustrates the basic point. It shows the emitter propagating along the $+z$ axis as a (nearly) localized classical particle. The dashed lines depict the small subset of other hard particles in the plasma which happen to pass close to the emitter during its flight and happen to interact with it when they do. Because of the localization of the emitter in space and time, and because of the local nature of the soft interactions (set by the Debye screening length $1/gT$), the interactions (for the particular background of hard particles shown) must happen in the order numbered in the diagram, regardless of when the collinear photon is emitted. That is, there can be no interference (at leading order in g) between the diagrams of figure 11 if the numbers 1 and 2 denote the fields generated

[7] Classical results become precise quantitatively in the limit that the photon energy is small compared to the emitter energy.

[8] In more detail, the transverse momenta in the wave packet will be order $\Delta p_\perp \sim \Delta p \sim gT$, both from the initial width as well as momentum transfer from scattering. The transverse spatial spread of the wave packet over time $\tau \sim 1/g^2T$ will then be $\tau \Delta p_\perp / p \sim 1/gT$, since $p \sim T$. There is also a longitudinal spread in the wave packet due to the effective thermal mass $m_\infty \sim gT$ of hard quarks, which gives a dispersion in velocities of order $\Delta v \sim \Delta(p/\sqrt{p^2 + m_\infty^2}) \sim m_\infty^2 \Delta p / p^3 \sim g^3$. The longitudinal spread of the wave packet due to this dispersion is then of order $\tau\, \Delta v \sim g/T$.

JHEP06(2002)030

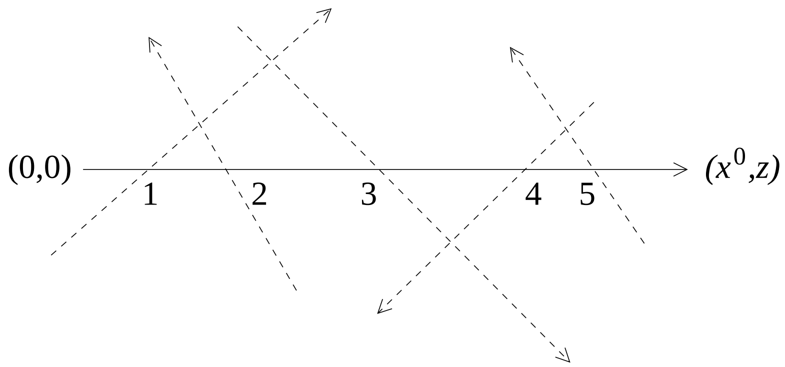

Figure 10: The emitter's trajectory, thought of as approximately classical, and the ordering in time and space this gives to its local interactions with scatterers (dashed lines).

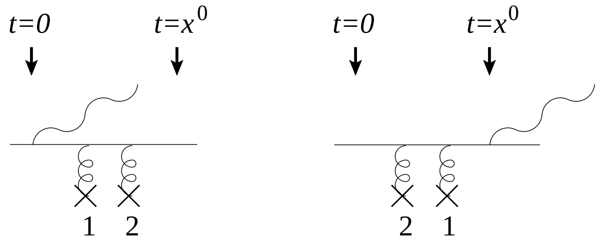

Figure 11: Two amplitudes which do not interfere (at leading order) because of mismatched order of encountering scatterers.

by two different scatterers. However, the diagrams of figure 12a and b could interfere. So could the diagrams of figure 12a and c, except that this particular interference vanishes when averaged over the randomness of the scatterers: the unmatched scatterer 4 could be a particle or anti-particle (for example), and a single insertion of its field in the product of amplitudes averages to zero by charge conjugation invariance. So, after averaging, non-zero contributions only arise from the cases where interactions with a given scatterer happen to appear twice in figure 9, with the interactions of the top and bottom rails consistently ordered in time and space. We can rewrite the random average of these figures in the form of figures 13 and 14, where the dashed lines indicate that the corresponding pair of A's have been replaced by the correlation $\langle\!\langle A_\mu A_\nu \rangle\!\rangle$. In our problem, this correlator is given by (2.4), but the argument we have used to arrive at figure 13 would also apply to *static* random scatterers, such as considered by Migdal, whenever one has a similar hierarchy of scales.

We should mention in passing that the condition that the entire wave packet remain well-localized, in all three dimensions, on a scale parametrically small compared to the mean separation between scattering events, is much stronger than necessary to argue that the interaction must be ordered in time (at leading order). Interactions are effectively ordered in time, and ladder diagrams dominate, in numerous other applications including the classic case of scattering from point-like static random impurities.[9]

[9]In this case, a localized wave packet impinging on a single scattering center will produce a scattered

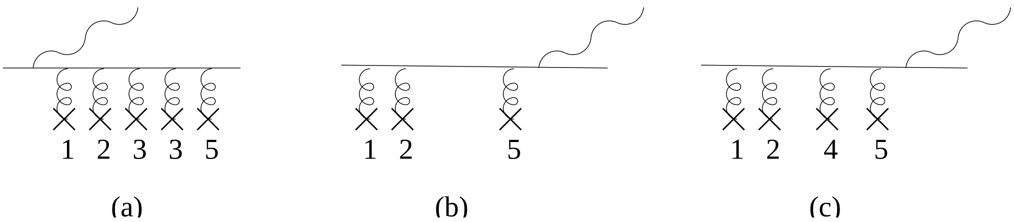

Figure 12: Amplitudes for which the time and space ordering of interactions is consistent.

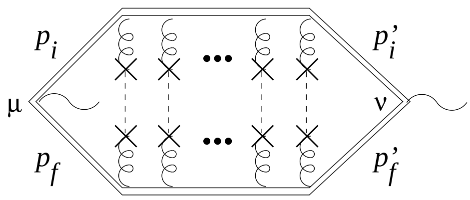

Figure 13: The product of amplitudes, as in figure 9, now averaged over random background fields. The dashed lines denote the independent correlations $\langle\!\langle AA \rangle\!\rangle$ of the background gauge fields. The double lines represent the resummed propagators of figure 14.

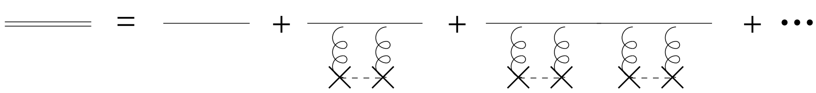

Figure 14: The resummation of self-energy insertions into the propagator.

The self-energy resummation on the top and bottom rails, involving insertions of the background field correlator as shown in figure 14, represents the inclusion of the thermal width Γ in the propagator of the emitting particle. In hot gauge theories, the thermal width of quasiparticles is dominated by soft scattering and is actually an infrared divergent quantity in perturbation theory. However, these divergences (which represent sensitivity to ultra-soft fluctuations) will turn out to cancel in our final result when combined with the correlations that connect the top and bottom rails. Our final formulas will be well behaved in the infrared.[10]

wave which resembles an outgoing spherical shell, with no localization in direction whatsoever. But as long as the temporal duration of the scattered wave (as it moves past a fixed location) is small compared to the mean time between collisions, multiply-scattered waves produced by scattering, in different orders, off a given set of scattering centers, will have negligible overlap and hence not interfere.

In particle-oriented language, all we are saying is that if a particle travels from some localized source to a localized detector by scattering twice, first off impurity A and then off B, its path length will be different than if it scatters first off B and then off A. As long as this difference in path length is large compared to the spatial extent of the wave packet, no significant interference can occur.

The basic criterion which is relevant here, and in all applications of kinetic theory, is that the mean time between collisions must be large compared to both the temporal duration of the initial wave packet (or $\hbar$ over its energy), and to the time duration of a single scattering event (as determined by the energy derivative of the scattering amplitude).

[10] "Rainbow" self-energy corrections, in which interactions with different scattering events are nested within each other, are suppressed for the same reason that crossed ladders are suppressed — because the mean time between $Q \sim gT$ interactions is parametrically large compared to the time duration of such

Before moving on to the evaluation of the ladder diagrams of figure 13, we may use the fuzzy classical particle picture to understand why the LPM effect depends crucially on the fact that the photon and the emitting particle move at or very close to the speed of light. If a particle of momentum p moving in the $+z$ direction emits a collinear photon of momentum k at time and position zero, then the subsequent positions of the particle and the photon at time t' will be

$$z_{\rm photon} \simeq v_\gamma\, t' \,, \qquad z_{\rm particle} \simeq v_{p-k}\, t' \,, \tag{2.10}$$

where v_γ is the velocity of the photon and v_p the velocity of the (quasi) particle with momentum p. If, on the other hand, the same particle doesn't emit the photon until time t, the subsequent positions will be

$$z_{\rm photon} \simeq v_p\, t + v_\gamma\, (t'-t) \,, \qquad z_{\rm particle} \simeq v_p\, t + v_{p-k}\, (t'-t) \,. \tag{2.11}$$

These two processes can interfere significantly only if the photon and particle trajectories are the same, up to the fuzziness Δx. That requires

$$v_\gamma t \simeq v_p t \simeq v_{p-k} t \,, \tag{2.12}$$

which is natural (that is, not suppressed by additional phase space restrictions) only if the particles are all ultrarelativistic.

3. Ladder diagrams as integral equations

3.1 Relativistic Schrödinger equation

A concise and convenient method for representing the propagation of nearly on-shell particles in a soft gauge background is with the relativistic one-particle Schrödinger equation. The free equation is

$$i\partial_t \psi = E_p \psi \,, \tag{3.1}$$

where $E_p = \sqrt{p^2+m^2}$ and m is the appropriate mass (in our case m_∞, which characterizes the in-medium dispersion correction of a hard fermion of negligible explicit mass). The corresponding retarded free propagator is just

$$G_0(P) = \frac{i}{p^0 - E_p + i\epsilon} \,, \tag{3.2}$$

and satisfies

$$\theta(t{-}t')\, \langle \mathbf{p}|U_0(t,t')|\mathbf{p}'\rangle = \int \frac{dp^0}{2\pi}\, e^{-ip^0(t-t')}\, G_0(P)\, \langle \mathbf{p}|\mathbf{p}'\rangle \,. \tag{3.3}$$

We will use the traditional normalization of one-particle quantum mechanics,

$$\langle \mathbf{p}|\mathbf{p}'\rangle = (2\pi)^3\, \delta^{(3)}(\mathbf{p}{-}\mathbf{p}') \,, \tag{3.4}$$

interactions. This is not true for ultra-soft interactions, for which a variety of diagrams are necessary when examining the diagrammatic basis for the cancellation responsible for insensitivity to ultra-soft scales. For details, see ref. [25]. In this paper, we ignore ultra-soft physics and simply check that our final answers are insensitive to it.

as opposed to the usual convention in relativistic field theory, which has an extra factor of $2E_p$ on the right hand side. Except for the change in normalization, $G_0(P)$ is just the positive-energy pole piece of the usual propagators of relativistic field theory (or, equivalently, the energy denominator of time-ordered perturbation theory when only single particle intermediate states contribute). The advantage of the description used here is that it does not depend on the spin or type of particle; it can be used to economically describe the propagation of hard scalars, fermions, or gauge bosons in soft background fields.

In a soft background gauge field (containing fluctuations on a scale $Q \sim gT \ll T \sim P$), the single-gluon vertex is just

$$ig\, v \cdot A\,, \tag{3.5}$$

up to corrections suppressed by $Q/P \sim g$, where v is defined by

$$v \equiv \frac{P}{p^0} = (1, \mathbf{v}) \simeq (1, \hat{\mathbf{p}})\,. \tag{3.6}$$

A simple, quick way to see this is to replace P by $P - gA$ in the Schrödinger equation (3.1) and propagator (3.2):

$$i\partial_t\, \psi + gA_0\psi = E_{\mathbf{p}-g\mathbf{A}}\, \psi\,. \tag{3.7}$$

Because the background field is soft, one may treat A and P as if they commute, since commutators will replace the operator P, whose relevant matrix elements are $O(T)$, by $Q \sim gT$, and hence only generate a subleading contribution. Expanding the equation to first order in A, one then obtains

$$i\partial_t\psi = (E_p - gv \cdot A)\, \psi + O(A^2)\,, \tag{3.8}$$

which gives the interaction (3.5). Only the "convective" contribution of the charged particle to the gauge current appears in the soft gluon vertex (3.5); the spin dependent contributions which would normally distinguish scalars, fermions, or gauge bosons are absent. Spin dependent contributions to the current are suppressed by an additional power of $Q/P \sim g$, and hence only generate sub-leading corrections to the propagation of a hard excitation through the soft background gauge field.

From the point of view of one-particle quantum mechanics, anti-particles are just another type of particle. The propagation of nearly on-shell anti-particles in a soft background field is also described by the propagator (3.2) and vertex (3.5) except that the gauge field A should be in the conjugate representation. Readers who prefer a discussion in terms of standard relativistic Feynman rules may refer to ref. [25].

3.2 The integral equation

The contribution to the leading-order photon emission rate from the sum of the ladder diagrams depicted in figure 13 may be expressed in terms of the solution to a suitable integral equation. Analogous summations of ladder diagrams are, of course, well known in many other contexts (such as the Bethe-Salpeter equation for bound states), although the form of the resulting integral equation intimately depends on the precise form of the propagators making up the rungs and side rails of the ladder diagrams, as well as the specific vertex factors at the ends of the diagrams.

The group structure of the diagrams of figure 13 is trivial: for every explicit power of g^2, there is also one factor of the quadratic Casimir C_R for the color representation R of the emitter. This Casimir is defined by $T^a_R T^a_R = C_R$ where T^a_R are the generators of the representation. For conventional quarks or anti-quarks in the fundamental representation of color SU(3), this Casimir is

$$C_R = \frac{4}{3} \qquad [\text{fundamental SU(3)}]\,. \tag{3.9}$$

Our first step will be to resum the self-energy insertions of figure 14 by switching from the propagator (3.2) to the resummed propagator

$$\frac{i}{p^0 - E_{\mathbf{p}} \pm i\Gamma_{\mathbf{p}}}\,, \tag{3.10}$$

where the $+$ sign gives the retarded propagator and the $-$ sign the advanced one. The width $\Gamma_{\mathbf{p}}$ is proportional to the imaginary part of the self-energy of the hard particle. The explicit form for this width is discussed below. The corresponding real part of the self energy is absorbed into $E_{\mathbf{p}}$. In fact the real part, unlike the imaginary part, is dominated by hard rather than soft collisions and cannot be directly computed in the soft background formalism we are using. Instead, it can be taken directly from the well-known hard thermal loop result, and just gives the usual effective thermal mass. For hard quarks, the effective energy is then

$$E_{\mathbf{p}} = \sqrt{p^2 + m_\infty^2}\,, \tag{3.11}$$

up to yet higher-order corrections, where [35, 36]

$$m_\infty^2 = \frac{1}{4}\, C_R\, g^2 T^2\,. \tag{3.12}$$

The sum of interferences represented by the diagrams of figure 13 may now be rewritten in terms of a linear integral equation as depicted in figure 15. To write this explicitly, it is convenient to work in frequency and momentum space. Consider the contribution to the correlator $W_{\mu\nu}$ from the $x^0 < 0$ portion of the x^0 integration in eq. (2.6).[11] If we rewrite the time evolution matrix elements in eq. (2.7) as $\langle\!\langle \langle \mathbf{p}_f | U(0,x^0) | \mathbf{p}'_f \rangle \, \langle \mathbf{p}_i | U(0,x^0) | \mathbf{p}'_i \rangle^* \rangle\!\rangle$ then we may use retarded propagators in evaluating these matrix elements. The resulting contribution to the current correlator, illustrated in figure 15, is

$$\int_P n(\mathbf{p}{+}\mathbf{k})\,[1 \pm n(\mathbf{p})]\,\langle \mathbf{p} | j_\mu(\mathbf{k}) | \mathbf{p}{+}\mathbf{k} \rangle^*\, \mathcal{S}_\nu(P;K)\,, \tag{3.13}$$

[11] We could equally well focus on the $x^0 > 0$ portion. As noted below, the two contributions are just complex conjugates of each other. It happens to be the $x^0 < 0$ portion which leads to the specific form of the integral equation derived in our earlier work [25].

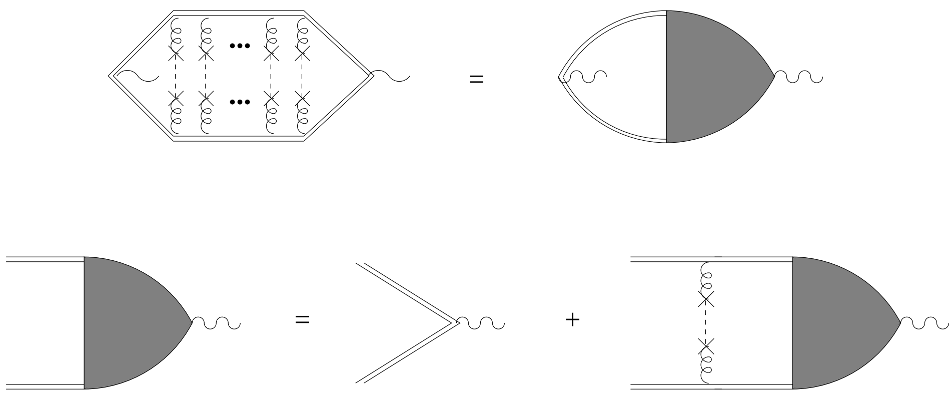

Figure 15: The leading-order contributions to the current-current correlator $W_{\mu\nu}$ expressed in terms of the solution to a linear integral equation.

where $\mathcal{S}_\nu(P;K)$, which represents the shaded vertex in figure 15, satisfies the integral equation[12]

$$\mathcal{S}_\nu(P;K) = \left(\frac{i}{(p^0+k^0)-E_{\mathbf{p+k}}+i\Gamma_{\mathbf{p+k}}}\right)^* \frac{i}{p^0-E_{\mathbf{p}}+i\Gamma_{\mathbf{p}}} \times \\ \times \left[\langle\mathbf{p}|j_\nu(\mathbf{k})|\mathbf{p+k}\rangle + g^2 C_R \int_Q \left\langle\!\!\left\langle [v_{\mathbf{p+k}}\cdot A(Q)]\,[v_{\mathbf{p}}\cdot A(Q)]^* \right\rangle\!\!\right\rangle \mathcal{S}_\nu(P{-}Q;K)\right]. \tag{3.14}$$

The color matrices and the momentum-conserving delta function $(2\pi)^4\delta^{(4)}(\cdots)$ are to be understood as already factored out of the $\langle\!\langle AA\rangle\!\rangle$ correlation in this (and subsequent) formulae. The $x^0>0$ region of the x^0 integration in (2.6) simply gives the complex conjugate (the replacement of retarded by advanced propagators), so that the total bremsstrahlung contribution, from a single carrier type and spin state, is

$$W^{\rm brem}_{\mu\nu}(K) = 2\,\mathrm{Re}\left[\int_P n(\mathbf{p+k})\,[1\pm n(\mathbf{p})]\,\langle\mathbf{p}|j_\mu(\mathbf{k})|\mathbf{p+k}\rangle^*\,\mathcal{S}_\nu(P;K)\right]. \tag{3.15}$$

Note that the photon four-momentum K is fixed, but the integral equation relates $\mathcal{S}_\nu(P;K)$ at different values of the four-vector P. In fact, at the order of interest, the dependence on P may be simplified. Let $p_\parallel$ represent the component of $\mathbf{p}$ in the direction $\mathbf{k}$ of the photon, and let $\mathbf{p}_\perp$ be the part of $\mathbf{p}$ perpendicular to $\mathbf{k}$. In our process, the momentum transfer is $O(gT)$, and so the relevant values of $\mathbf{p}_\perp$ are $O(gT)$. Expanding in both $\mathbf{p}_\perp$ and the thermal mass m_∞, one has

$$p^0 - E_{\mathbf{p}} + i\Gamma_{\mathbf{p}} \simeq (p^0-p_\parallel) - \frac{p_\perp^2+m_\infty^2}{2p_\parallel} + i\Gamma_{\mathbf{p}}\,, \tag{3.16}$$

$$(p^0+k^0) - E_{\mathbf{p+k}} + i\Gamma_{\mathbf{p+k}} \simeq (p^0-p_\parallel) - \frac{p_\perp^2+m_\infty^2}{2(p_\parallel+k)} + i\Gamma_{\mathbf{p+k}}\,, \tag{3.17}$$

[12] $\mathcal{S}_\nu$ here is analogous to the combination $\mathcal{FD}_\nu$ of ref. [25]. We have chosen our conventions for defining $\mathcal{S}_\nu$ so that later equations will closely resemble those of refs. [25, 26].

where we have assumed that the photon is on-shell, and that $p_{\|} > 0$ so that the photon is traveling in the same direction as the emitter. The last two terms in both equations are $O(g^2T)$, and so each of the propagators will be suppressed unless $p^0 - p_{\|}$ is also $O(g^2T)$.[13] If $\mathcal{S}_\nu(P;K)$ is only ever going to be integrated against functions that are smooth on the scale of $O(g^2T)$ variations in $p^0 - p_{\|}$, then one may approximate

$$\left(\frac{i}{(p^0+k^0)-E_{\mathbf{p}+\mathbf{k}}+i\Gamma_{\mathbf{p}+\mathbf{k}}}\right)^* \frac{i}{p^0-E_{\mathbf{p}}+i\Gamma_{\mathbf{p}}} \simeq \frac{2\pi i\,\delta(p^0-p_{\|})\,\theta(p_{\|})}{(E_{\mathbf{p}+\mathbf{k}}+i\Gamma_{\mathbf{p}+\mathbf{k}})-(k^0+E_{\mathbf{p}}-i\Gamma_{\mathbf{p}})}$$
$$\simeq \frac{2\pi\,\delta(p^0-p_{\|})\,\theta(p_{\|})}{i\,\delta E+(\Gamma_{\mathbf{p}+\mathbf{k}}+\Gamma_{\mathbf{p}})}\,, \tag{3.18}$$

where
$$\delta E \equiv \frac{k\,(p_\perp^2+m_\infty^2)}{2p_{\|}\,(k+p_{\|})} \simeq k^0+E_{\mathbf{p}}-E_{\mathbf{p}+\mathbf{k}}\,. \tag{3.19}$$

This is commonly known as the pinching pole approximation, and in our analysis is justified for computing the rate at leading order in g. Making this substitution into the integral equation (3.14), one sees that the resulting solution will have the form

$$\mathcal{S}_\nu(P;K) = S_\nu(\mathbf{p};K)\,2\pi\,\delta(p^0-p_{\|})\,\theta(p_{\|})\,. \tag{3.20}$$

Inserting this form, and rewriting

$$\delta(p^0-p_{\|})\,\delta\big((p^0-q^0)-(p_{\|}-q_{\|})\big) = \delta(p^0-p_{\|})\,\delta(q^0-q_{\|})\,, \tag{3.21}$$

one finds

$$W_{\mu\nu}^{\rm brem}(K) = 2\,\mathrm{Re}\int_{\mathbf{p}} n(\mathbf{p}{+}\mathbf{k})\,[1\pm n(\mathbf{p})]\,\langle\mathbf{p}|j_\mu(\mathbf{k})|\mathbf{p}{+}\mathbf{k}\rangle^*\,S_\nu(\mathbf{p};\mathbf{k})\,\theta(p_{\|}), \tag{3.22}$$

where

$$S_\nu(\mathbf{p};\mathbf{k}) = \frac{1}{i\delta E+(\Gamma_{\mathbf{p}+\mathbf{k}}+\Gamma_{\mathbf{p}})}\times \tag{3.23}$$
$$\times\left[\langle\mathbf{p}|j_\nu(\mathbf{k})|\mathbf{p}{+}\mathbf{k}\rangle + g^2C_R\int_Q 2\pi\,\delta(q^0-q_{\|})\,\left\langle\!\!\left\langle [v_{\mathbf{p}+\mathbf{k}}\cdot A(Q)]\,[v_{\mathbf{p}}\cdot A(Q)]^*\right\rangle\!\!\right\rangle\,S_\nu(\mathbf{p}{-}\mathbf{q};\mathbf{k})\right].$$

In terms of the current matrix elements appearing in the original definition (2.6), the function $S_\nu(\mathbf{p};\mathbf{k})$ is given by that portion of the time-evolved off-diagonal matrix element of the current, evaluated in the fluctuating background gauge field, which is phase-coherent with the emitted photon. That is, to leading order in $g_{\rm s}$,

$$\int d^4x\;\theta(-x^0)\,e^{-iKx}\,\left\langle\!\!\left\langle\langle\mathbf{p}|j_\nu(x)|\mathbf{p}{+}\mathbf{k}\rangle\right\rangle\!\!\right\rangle = S_\nu(\mathbf{p};\mathbf{k})\,\theta(p_{\|})\,. \tag{3.24}$$

Time evolution is, of course, implicit in $j_\nu(x) = j_\nu(x^0,\mathbf{x}) = U(0,x^0)\,j_\nu(\mathbf{x})\,U(x^0,0)$.

[13] If $p_{\|} < 0$, then the two propagators are peaked near $p^0 = -p_{\|}$ and $p^0+k = |p_{\|}+k|$, and it is impossible for both propagators to simultaneously be (nearly) on-shell. Hence, only the region $p_{\|} > 0$ contributes to the leading-order bremsstrahlung rate.

In the interaction term of eq. (3.23) one may, at leading order, replace $v_{\mathbf{p}} \cdot A$ by

$$A^- \equiv A^0 - A_{\|} \tag{3.25}$$

and rewrite the integral equation in the form

$$\begin{aligned}\langle \mathbf{p}|j_\nu(\mathbf{k})|\mathbf{p}{+}\mathbf{k}\rangle &= [i\,\delta E + (\Gamma_{\mathbf{p}+\mathbf{k}} + \Gamma_{\mathbf{p}})]\, S_\nu(\mathbf{p};\mathbf{k}) - \\ &- g^2 C_R \int_Q 2\pi\, \delta(q^0{-}q_{\|}) \left\langle\!\!\left\langle A^-(Q)\, [A^-(Q)]^* \right\rangle\!\!\right\rangle S_\nu(\mathbf{p}{-}\mathbf{q};\mathbf{k})\,.\end{aligned} \tag{3.26}$$

As it stands, this integral equation mixes together different values of $p_{\|}$ (as well as different $\mathbf{p}_\perp$) in the argument of $S(\mathbf{p};\mathbf{k})$, due to the $O(gT)$ momentum transfers in the interaction term. The characteristic size of $p_{\|}$ for a hard quasiparticle is $O(T)$, and no elements in the equation are sensitive (at leading order) to gT variations in $p_{\|}$. Consequently, we can treat $p_{\|}$ as fixed inside the interaction term,[14] replacing the equation by

$$\begin{aligned}\langle \mathbf{p}|j_\nu(\mathbf{k})|\mathbf{p}{+}\mathbf{k}\rangle &= [i\,\delta E + (\Gamma_{\mathbf{p}+\mathbf{k}} + \Gamma_{\mathbf{p}})]\, S_\nu(\mathbf{p}_\perp;p_{\|},\mathbf{k}) - \\ &- g^2 C_R \int_Q 2\pi\, \delta(q^0{-}q_{\|}) \left\langle\!\!\left\langle A^-(Q)\, [A^-(Q)]^* \right\rangle\!\!\right\rangle S_\nu(\mathbf{p}_\perp{-}\mathbf{q}_\perp;p_{\|},\mathbf{k})\,.\end{aligned} \tag{3.27}$$

This is now a linear integral equation in $\mathbf{p}_\perp$ space, for fixed values of $p_{\|}$ and $\mathbf{k}$.

One remaining complication is that both the width $\Gamma_{\mathbf{p}}$ and the total scattering cross section have infrared divergences in our approximations, proportional to the $Q \to 0$ divergence of $\int_Q 2\pi\delta(q^0{-}q_{\|})\,\langle\!\langle A^-(Q)[A^-(Q)]^*\rangle\!\rangle$. This divergence of $\Gamma_{\mathbf{p}}$ in HTL perturbation theory is well known [37], arises from collisions via the exchange of unscreened low-frequency magnetic gluons, and is a symptom of sensitivity to ultra-soft non-perturbative magnetic physics at the momentum scale g^2T. But this apparent infrared sensitivity is actually illusory in our problem, as may be seen by rewriting the width in a form similar to the interaction term in eq. (3.27). The width comes from the imaginary parts of the self-energy insertions in figure 14 for nearly on-shell particles and, to leading order, is given by

$$\begin{aligned}\Gamma_{\mathbf{p}} &= \mathrm{Im}\left[i g^2 C_R \int_Q \frac{i}{(p^0{-}q^0) - E_{\mathbf{p}-\mathbf{q}} + i\epsilon} \left\langle\!\!\left\langle A^-(Q)\, A^-(-Q) \right\rangle\!\!\right\rangle \right]_{p^0=E_{\mathbf{p}}} \\ &\simeq g^2 C_R \int_Q \pi\delta(q^0{-}q_{\|}) \left\langle\!\!\left\langle A^-(Q)\, [A^-(Q)]^* \right\rangle\!\!\right\rangle.\end{aligned} \tag{3.28}$$

Substituting this into (3.27), one obtains the infrared-safe equation

$$\begin{aligned}\langle \mathbf{p}|j_\nu(\mathbf{k})|\mathbf{p}{+}\mathbf{k}\rangle = i\,\delta E\, S_\nu(\mathbf{p}_\perp;p_{\|},\mathbf{k}) + g^2 C_R \int_Q 2\pi\, \delta(q^0{-}q_{\|}) \left\langle\!\!\left\langle A^-(Q)\, [A^-(Q)]^* \right\rangle\!\!\right\rangle \times \\ \times \left[S_\nu(\mathbf{p}_\perp;p_{\|},\mathbf{k}) - S_\nu(\mathbf{p}_\perp{-}\mathbf{q}_\perp;p_{\|},\mathbf{k})\right].\end{aligned} \tag{3.29}$$

[14] This may be argued in more detail as follows. Given the linearity of the integral equation, one could multiply the source $\langle \mathbf{p}|j_\nu(\mathbf{k})|\mathbf{p}{+}\mathbf{k}\rangle$ in (3.26) by $\delta(p_{\|}{-}p_{\|}')$, at the cost of introducing an integral over $p_{\|}'$ in the final expression (3.22). The resulting solution to the integral equation would then have its dominant support on values of $p_{\|}$ which differ from $p_{\|}'$ only by total momentum transfers of $O(gT)$. Because the $\langle \mathbf{p}|j_\nu(\mathbf{k})|\mathbf{p}{+}\mathbf{k}\rangle^*\,\theta(p_{\|})$ factor in (3.22) is smooth in $p_{\|}$ (for $p_{\|}$ of order T), no error is made at leading order if $p_{\|}$ is replaced by $p_{\|}'$ in these terms. If the modified (3.26) is then integrated over $p_{\|}$, and $\int dp_{\|}\, S(\mathbf{p};p_{\|}',\mathbf{k})$ is renamed $S(\mathbf{p}_\perp;p_{\|}',\mathbf{k})$, one arrives at eqs. (3.22) and (3.27).

We may also tidy up the expression for $W_{\mu\nu}$ by noting that $n(p) \simeq n(p_\parallel)$ [since $\mathbf{p}_\perp$ is $O(gT)$], so that to leading order

$$W_{\mu\nu}^{\rm brem}(K) = 2\,{\rm Re} \int_{\mathbf{p}} n(p_\parallel{+}k)\,[1 \pm n(p_\parallel)]\,\langle \mathbf{p}|j_\mu(\mathbf{k})|\mathbf{p}{+}\mathbf{k}\rangle^*\, S_\nu(\mathbf{p}_\perp;p_\parallel,\mathbf{k})\,\theta(p_\parallel)\,. \tag{3.30}$$

3.3 Current matrix elements

The current matrix element $\langle \mathbf{p}|j_\mu(\mathbf{k})|\mathbf{p}{+}\mathbf{k}\rangle$ is the only ingredient of our equations that depends on the nature of the emitter (i.e., scalar or fermion). Since $\mathbf{p}_\perp$ is parametrically small compared to $p_\parallel$, it is sufficient to evaluate these matrix elements in the limit of small transverse momentum. We only need the transverse components of j_μ because the currents are dotted into photon polarization vectors in eq. (2.2). By rotational invariance about the $\mathbf{k}$ axis, these must be proportional to $\mathbf{p}_\perp$. Let qe denote the electric charge of the emitting particle (so that up quarks, for example, have $q = 2/3$). Then in the small $\mathbf{p}_\perp$ limit, the transverse current matrix element takes the form

$$\langle \mathbf{p}|\mathbf{j}_\perp(\mathbf{k})|\mathbf{p}{+}\mathbf{k}\rangle \simeq 2qe\,\mathbf{p}_\perp\,\mathcal{J}_{p_\parallel \leftarrow p_\parallel + k}, \tag{3.31}$$

where we have chosen to factor out the charge of the emitter. The explicit form of the "splitting function" $\mathcal{J}_{p_\parallel \leftarrow p_\parallel + k}$, which depends on $p_\parallel$ and k as well as the spin of the emitter, will be discussed momentarily. Given the linearity of the integral equation (3.29) (and the fact that it only couples different values of $\mathbf{p}_\perp$, not $p_\parallel$), we can factor out all dependence on the emitter type by redefining the transverse part of $S_\nu(\mathbf{p}_\perp;p_\parallel,k)$ as

$$\mathbf{S}_\perp(\mathbf{p}_\perp;p_\parallel,\mathbf{k}) = qe\,\mathcal{J}_{p_\parallel \leftarrow p_\parallel + k}\,\mathbf{f}(\mathbf{p}_\perp;p_\parallel,\mathbf{k}) \tag{3.32}$$

to obtain

$$\sum_a \epsilon_a^{\mu *}\epsilon_a^{\nu} W_{\mu\nu}^{\rm brem}(K) = 2(qe)^2\,{\rm Re} \int_{\mathbf{p}} n(p_\parallel{+}k)\,[1{\pm}n(p_\parallel)]\,|\mathcal{J}_{p_\parallel \leftarrow p_\parallel + k}|^2\; 2\mathbf{p}_\perp\cdot\mathbf{f}(\mathbf{p}_\perp;p_\parallel,\mathbf{k})\,\theta(p_\parallel), \tag{3.33}$$

where $\mathbf{f}(\mathbf{p}_\perp;p_\parallel,\mathbf{k})$ is the solution to[15]

$$\begin{aligned} 2\mathbf{p}_\perp &= i\,\delta E\,\mathbf{f}(\mathbf{p}_\perp;p_\parallel,\mathbf{k}) + g^2 C_R \int_Q 2\pi\,\delta(q^0{-}q_\parallel)\,\Big\langle\!\Big\langle A^-(Q)\,[A^-(Q)]^* \Big\rangle\!\Big\rangle \times \\ &\qquad\qquad \times \big[\mathbf{f}(\mathbf{p}_\perp;p_\parallel,\mathbf{k}) - \mathbf{f}(\mathbf{p}_\perp{-}\mathbf{q}_\perp;p_\parallel,\mathbf{k})\big]\,. \end{aligned} \tag{3.34}$$

This gives the result for bremsstrahlung production from a single type and spin (and initial color) of charged particle in a way that clearly isolates (i) the dependence on the type of the particle in the splitting factor $|\mathcal{J}_{p_\parallel \leftarrow p_\parallel + k}|^2$, and (ii) the dependence on the details of the frequency-dependent correlation of the background field in the correlator $\langle\!\langle AA \rangle\!\rangle$.

If the charge carriers are scalars, one would have

$$\langle \mathbf{p}|\mathbf{j}_\perp(\mathbf{k})|\mathbf{p}{+}\mathbf{k}\rangle = qe\,\frac{(2\mathbf{p}+\mathbf{k})_\perp}{(2E_{\mathbf{p}})^{1/2}(2E_{\mathbf{p}+\mathbf{k}})^{1/2}} \simeq qe\,\frac{\mathbf{p}_\perp}{[p_\parallel(p_\parallel+k)]^{1/2}}\,. \tag{3.35}$$

[15] Rotation invariance about $\mathbf{k}$ implies that $\mathbf{f}(\mathbf{p}_\perp;p_\parallel,\mathbf{k})$ must equal $\mathbf{p}_\perp$ times a scalar function of $|\mathbf{p}_\perp|$, $p_\parallel$, and k. (See ref. [26].) But the resulting integral equation (3.34) is more compact if $\mathbf{f}(\mathbf{p}_\perp;p_\parallel,\mathbf{k})$ is left as a vector function.

JHEP06(2002)030

The numerator in the middle expression is the usual photon vertex in relativistic normalization, while the denominator arises from our use of a non-relativistic normalization (3.4) for our states. Making a similar calculation for fermions, one obtains[16]

$$|\mathcal{J}_{p_\parallel \leftarrow p_\parallel + k}|^2 = \begin{cases} \dfrac{1}{4p_\parallel\,(p_\parallel{+}k)}, & \text{scalars;} \\ \dfrac{{p_\parallel}^2 + (p_\parallel{+}k)^2}{8{p_\parallel}^2(p_\parallel{+}k)^2}, & \text{fermions.} \end{cases} \tag{3.36}$$

This result can also be expressed in terms of the leading-order Altarelli-Parisi (or DGLAP) splitting functions for (hard) photon bremsstrahlung from a charged particle q,

$$|\mathcal{J}_{p_\parallel \leftarrow p_\parallel + k}|^2 = \left. \frac{k\, P_{q(\gamma)\leftarrow q}(z)}{8{p_\parallel}^2(p_\parallel{+}k)} \right|_{z=p_\parallel/(p_\parallel+k)}, \tag{3.37}$$

where[17]

$$P_{q(\gamma)\leftarrow q}(z) = \begin{cases} \dfrac{2z}{1-z}, & \text{scalars;} \\ \dfrac{1+z^2}{1-z}, & \text{fermions,} \end{cases} \tag{3.38}$$

for $z < 1$.

3.4 Relationship to Migdal's equation

Let us note in passing the relationship of our result to similar equations written by Migdal [29, 30] for the case of hard bremsstrahlung during electron scattering from the static Coulomb fields of randomly distributed atoms. If the background were static, we could write

$$\Big\langle\!\!\Big\langle A^-(Q)\,[A^-(Q)]^* \Big\rangle\!\!\Big\rangle = 2\pi\delta(q^0)\, \Big\langle\!\!\Big\langle A^-(\mathbf{q})\,[A^-(\mathbf{q})]^* \Big\rangle\!\!\Big\rangle, \tag{3.39}$$

and the collision term in (3.29) would then become

$$g^2 C_R \int_{\mathbf{q}} 2\pi\, \delta(q_\parallel)\, \Big\langle\!\!\Big\langle A^-(\mathbf{q})\,[A^-(\mathbf{q})]^* \Big\rangle\!\!\Big\rangle\, [S_\nu(\mathbf{p}_\perp; p_\parallel, \mathbf{k}) - S_\nu(\mathbf{p}_\perp{-}\mathbf{q}_\perp; p_\parallel, \mathbf{k})]\,. \tag{3.40}$$

Migdal has an equivalent expression (ref. [30, eq. (9)]) but with $\delta(q_\parallel)$ replaced by

$$\frac{1}{2}\,\delta(E_{\mathbf{p}+\mathbf{q}} - E_{\mathbf{p}}) + \frac{1}{2}\,\delta(E_{\mathbf{p}+\mathbf{k}+\mathbf{q}} - E_{\mathbf{p}+\mathbf{k}}). \tag{3.41}$$

At leading order, however, both of these delta functions are equivalent to $\delta(q_\parallel)$, and so our result reduces to Migdal's in this special case.

[16]See, for example, ref. [25] for more detail, bearing in mind the change to the non-relativistic normalization used here.

[17]$P_{q(g)\leftarrow q} = C_R[(1+z^2)/(1-z)_+ + \frac{3}{2}\,\delta(1-z)]$ is the standard result for gluon bremsstrahlung from a quark. The corresponding splitting function for photon production is obtained by replacing C_R by 1. The treatment of the soft photon singularities at $z{=}1$ is not relevant to us, since our photons are hard; hence we may ignore the $\delta(1{-}z)$ and the endpoint prescription on the $(1{-}z)$ denominator.

Migdal went on to solve his equation in the approximation that the LPM effect was parametrically large — roughly, that $\delta E \ll \Gamma_{\mathbf{p}}$ (or equivalently that the formation time was large compared to the mean free collision time), in which case it turned out he was able to expand in the logarithm of the ratio,[18] $\ln(\Gamma_{\mathbf{p}}/\delta E)$. In our application, δE and $\Gamma_{\mathbf{p}}$ are of the same parametric order, and such an expansion is not useful.

4. Pair annihilation

The treatment of pair annihilation is very closely related to that of bremsstrahlung — a fact which is slightly obscured in the present time-ordered discussion but is more manifest in our original treatment of ref. [25]. The contribution to the current-current correlator $W_{\mu\nu}$ due to pair annihilation, in a form analogous to eq. (2.6) for bremsstrahlung, is

$$W^{\rm pair}_{\mu\nu}(K) = \left\langle\!\!\left\langle \int d^4x\, e^{-iKx} \int_{\mathbf{p}\bar{\mathbf{p}}} n(p)\, n(\bar p)\, \langle \mathbf{p}\bar{\mathbf{p}}|j_\mu(0)|{\rm vac}\rangle\, \langle {\rm vac}|j_\nu(x)|\mathbf{p}\bar{\mathbf{p}}\rangle \right\rangle\!\!\right\rangle . \tag{4.1}$$

Using the fact that particles propagate independently in our approximation (the only interactions are with the background field), this can be written in terms of one-particle evolution amplitudes as

$$\begin{aligned}\int d^4x\, e^{-iKx} \int_{\mathbf{p}\mathbf{p}'\bar{\mathbf{p}}\bar{\mathbf{p}}'} n(p)\, n(\bar p) \left\langle\!\!\left\langle \langle \mathbf{p}\bar{\mathbf{p}}|j_\mu(0)|{\rm vac}\rangle\, \langle {\rm vac}|j_\nu(\mathbf{x})|\mathbf{p}'\bar{\mathbf{p}}'\rangle\, \langle \mathbf{p}'\bar{\mathbf{p}}'|U(x^0,0)|\mathbf{p}\bar{\mathbf{p}}\rangle \right\rangle\!\!\right\rangle = \\ = \int d^4x\, e^{-iKx} \int_{\mathbf{p}\mathbf{p}'\bar{\mathbf{p}}\bar{\mathbf{p}}'} n(p)\, n(\bar p)\ \langle \mathbf{p}\bar{\mathbf{p}}|j_\mu(0)|{\rm vac}\rangle\, \langle {\rm vac}|j_\nu(\mathbf{x})|\mathbf{p}'\bar{\mathbf{p}}'\rangle \times \\ \times \left\langle\!\!\left\langle \langle \mathbf{p}'|U(x^0,0)|\mathbf{p}\rangle\, \langle \bar{\mathbf{p}}'|U(x^0,0)|\bar{\mathbf{p}}\rangle \right\rangle\!\!\right\rangle .\end{aligned} \tag{4.2}$$

Translation invariance now gives the momentum conservation constraint

$$\mathbf{k} = \mathbf{p} + \bar{\mathbf{p}} = \mathbf{p}' + \bar{\mathbf{p}}' . \tag{4.3}$$

Note that we have ignored processes where the particle and antiparticle interact directly with each other via gluon exchange, rather than with the random background field created by other color charge carriers in the plasma. Such processes are sub-leading in g, as are vertex corrections to bremsstrahlung.[19]

[18] At very high energies, this logarithm is modified in Midgal's analysis by the finite nuclear size of the atomic scatterer, which is also irrelevant to our application.

[19] A simple qualitative way to understand this is to consider the typical interaction energy times the photon formation time (which, among other things, is the time the annihilating pair spend within a Debye screening length of each other) in the center of mass frame of the almost-collinear annihilating pair. If this product is small compared to 1, then the effect of direct gluon interactions between the pair is suppressed. The formation time is $1/g^2T$ in the plasma frame, and becomes smaller by a factor of $m_\infty/T \sim g$ when boosted to the center-of-mass frame, giving $1/gT$. The characteristic distance between the pair over the formation time is $r \sim 1/gT$, giving a characteristic potential energy of order $g^2/r \sim g^3T$. The product is then order $g^2 \ll 1$. For comparison, the interaction time and distance for interaction with a random colored particle are both order $1/gT$, and the energy-time product is again g^2. But the pair encounters $N \sim 1/g^4$

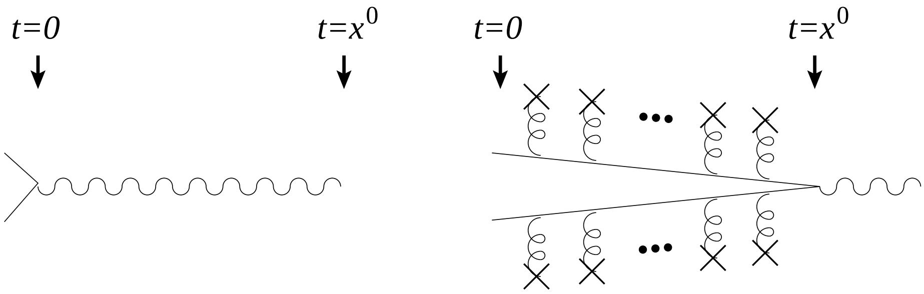

Figure 16: Two (time-ordered) diagrams whose interference contributes to the pair annihilation rate.

The pair annihilation contribution to the current correlator $W_{\mu\nu}$ represents the interference of the two processes shown in figure 16. The interference of these amplitudes can again be depicted by a diagram like figure 9, but now the interpretation is slightly different. The left photon vertex represents the conjugate of the first diagram of figure 16, and everything else represents the second diagram of figure 16. The same time and space ordering considerations discussed for bremsstrahlung again imply that the only relevant correlations at leading order are those depicted by figure 13. The resulting integral equation is closely related to the one for bremsstrahlung:

$$W_{\mu\nu}^{\rm pair}(K) = 2\,{\rm Re}\int_P n(\mathbf{k}{-}\mathbf{p})\,n(\mathbf{p})\,\langle{\rm vac}|j_\mu(\mathbf{k})|\mathbf{p},\mathbf{k}{-}\mathbf{p}\rangle^*\,\widetilde{\mathcal{S}}_\nu(P;K)\,, \tag{4.4}$$

with[20]

$$\begin{aligned}\widetilde{\mathcal{S}}_\nu(P;K) = {} & \left(\frac{i}{(k^0{-}p^0) - E_{\mathbf{k}-\mathbf{p}} + i\Gamma_{\mathbf{k}-\mathbf{p}}}\right)^*\left(\frac{i}{p^0 - E_{\mathbf{p}} + i\Gamma_{\mathbf{p}}}\right)^* \times \\ & \times\left[\langle\mathbf{p},\mathbf{k}{-}\mathbf{p}|j_\nu(\mathbf{k})|{\rm vac}\rangle + g^2 C_R\int_Q \left\langle\!\!\left\langle [v_{\mathbf{k}-\mathbf{p}}\cdot A(Q)]\,[v_{\mathbf{p}}\cdot A(-Q)]\right\rangle\!\!\right\rangle \widetilde{\mathcal{S}}_\nu(P{-}Q;K)\right].\end{aligned} \tag{4.5}$$

The pinching pole approximation is now

$$\begin{aligned}\left[\frac{i}{(k^0{-}p^0) - E_{\mathbf{k}-\mathbf{p}} + i\Gamma_{\mathbf{k}-\mathbf{p}}}\right]^*\left[\frac{i}{p^0 - E_{\mathbf{p}} + i\Gamma_{\mathbf{p}}}\right]^* & \simeq \frac{2\pi i\,\delta(p^0{-}p_\parallel)\,\theta(p_\parallel)\,\theta(k{-}p_\parallel)}{(E_{\mathbf{k}-\mathbf{p}} + i\Gamma_{\mathbf{k}-\mathbf{p}}) + (E_{\mathbf{p}} + i\Gamma_{\mathbf{p}}) - k^0} \\ & \simeq \frac{2\pi\,\delta(p^0{-}p_\parallel)\,\theta(p_\parallel)\,\theta(k{-}p_\parallel)}{i\widetilde{\delta E} + (\Gamma_{\mathbf{k}-\mathbf{p}} + \Gamma_{\mathbf{p}})}\,,\end{aligned} \tag{4.6}$$

where

$$\widetilde{\delta E} \equiv -\left[\frac{p_\perp^2 + m_\infty^2}{2}\right]\left[\frac{k}{p_\parallel\,(k{-}p_\parallel)}\right] \simeq k^0 - E_{\mathbf{k}-\mathbf{p}} - E_{\mathbf{p}}\,. \tag{4.7}$$

such random particles during the formation time [number density T^3 times Debye screening volume $1/(gT)^3$ times formation time $1/g^2T$ divided by time $1/gT$ interacting with each particle]. These encounters will on average cancel each other in their effects except for statistical fluctuations, which will enhance our g^2 contribution per random encounter by $\sqrt{N}$ to give a net, unsuppressed effect of $g^2\sqrt{N} \sim 1$.

[20] A note on signs: the i's from the two soft gluon interactions cancel the minus sign associated with the fact that the color generators for the anti-particle are $-T^*$ instead of T.

The same simplifications as for bremsstrahlung then reduce these expressions to

$$\sum_a \epsilon_a^{\mu *}\epsilon_a^{\nu}\, W^{\rm pair}_{\mu\nu}(K) \;=\; 2\,(qe)^2\, {\rm Re} \int_{\mathbf p} n(k{-}p_\parallel)\,[1\pm n(p_\parallel)]\, |\mathcal{J}_{{\rm vac}\leftarrow p_\parallel, k-p_\parallel}|^2 \times$$
$$\times\, 2\mathbf{p}_\perp \cdot \widetilde{\mathbf f}(\mathbf{p}_\perp; p_\parallel, \mathbf{k})\,\theta(p_\parallel)\,\theta(k{-}p_\parallel)\,, \qquad (4.8)$$

and

$$2\mathbf{p}_\perp \;=\; i\,\widetilde{\delta E}\,\widetilde{\mathbf f}(\mathbf{p}_\perp; p_\parallel, \mathbf{k}) + g^2 C_R \int_Q 2\pi\,\delta(q^0{-}q_\parallel) \left\langle\!\!\left\langle A^-(Q)\,[A^-(Q)]^* \right\rangle\!\!\right\rangle \times$$
$$\times \Big[\widetilde{\mathbf f}(\mathbf{p}_\perp; p_\parallel, \mathbf{k}) - \widetilde{\mathbf f}(\mathbf{p}_\perp{-}\mathbf{q}_\perp; p_\parallel, \mathbf{k})\Big]\,, \qquad (4.9)$$

where we have defined the small $\mathbf{p}_\perp$ limit

$$\langle {\rm vac}| j_\mu(\mathbf{k}) |\mathbf{p}, \mathbf{p}{-}\mathbf{k}\rangle \simeq 2qe\, \mathbf{p}_\perp\, \mathcal{J}_{{\rm vac}\leftarrow p_\parallel, k-p_\parallel} \qquad (4.10)$$

analogous to eq. (3.31). These “joining functions” are given by

$$|\mathcal{J}_{{\rm vac}\leftarrow p_\parallel, k-p_\parallel}|^2 = \begin{cases} \dfrac{1}{4p_\parallel\,(k{-}p_\parallel)}\,, & \text{scalars;} \\[2ex] \dfrac{{p_\parallel}^2 + (k{-}p_\parallel)^2}{8[p_\parallel\,(k{-}p_\parallel)]^2}\,, & \text{fermions;} \end{cases} \qquad (4.11)$$

which is the same, up to an overall sign, as taking $p_\parallel \to -p_\parallel$ in the bremsstrahlung formula (3.36).

The results (4.8) and (4.9) can be cast into exactly the same form as the bremsstrahlung results (3.33) and (3.34), with the only difference being a factor of $\theta(-p_\parallel)\,\theta(k+p_\parallel)$ in eq. (4.8) instead of $\theta(p_\parallel)$. To see this, everywhere redefine $\mathbf{p} \to -\mathbf{p}$ in eq. (4.8), including $p_\parallel \to -p_\parallel$. Then define

$$\mathbf{f}(\mathbf{p}_\perp, p_\parallel; \mathbf{k}) \equiv \widetilde{\mathbf f}(-\mathbf{p}_\perp, -p_\parallel; \mathbf{k})\,. \qquad (4.12)$$

The equivalence is completed by the identity

$$n(-p_\parallel) = \mp[1 \pm n(p_\parallel)] \qquad (4.13)$$

and the relationship between the squares of current matrix elements (3.36) and (4.11) just noted.

5. Final formulas for photon emission

To produce a final formula for the leading order contribution to hard photon production from near collinear bremsstrahlung and pair annihilation, we just need to combine the defining relation (2.1) with the result (3.34) for bremsstrahlung and the result (4.8) for pair annihilation, transformed as just discussed, and finally sum over the colors, spins, and flavors of possible emitters. The final result can be neatly packaged in the form

$$\frac{d\Gamma^{\rm LPM}_\gamma}{d^3\mathbf{k}} = d_R\, \frac{\alpha_{\rm EM}}{4\pi^2 k} \left(\sum_s N_s\, q_s^2\right) \int_{-\infty}^{+\infty} \frac{dp_\parallel}{2\pi} \int \frac{d^2\mathbf{p}_\perp}{(2\pi)^2}\, n_{\rm f}(p_\parallel{+}k)\,[1{-}n_{\rm f}(p_\parallel)] \times$$
$$\times\, |\mathcal{J}_{p_\parallel \leftarrow p_\parallel + k}|^2\; 2\mathbf{p}_\perp \cdot {\rm Re}\,\mathbf{f}(\mathbf{p}_\perp; p_\parallel, \mathbf{k})\,, \qquad (5.1)$$

where $\mathbf{f}(\mathbf{p}_\perp; p_\parallel, \mathbf{k})$ satisfies the integral equation (3.34), repeated here for convenience,

$$2\mathbf{p}_\perp = i\,\delta E\,\mathbf{f}(\mathbf{p}_\perp; p_\parallel, \mathbf{k}) + g^2 C_R \int_Q 2\pi\,\delta(q^0 - q_\parallel) \left\langle\!\!\left\langle A^-(Q)\,[A^-(Q)]^* \right\rangle\!\!\right\rangle \times \\ \times \left[\mathbf{f}(\mathbf{p}_\perp; p_\parallel, \mathbf{k}) - \mathbf{f}(\mathbf{p}_\perp - \mathbf{q}_\perp; p_\parallel, \mathbf{k})\right], \tag{5.2}$$

and δE is defined in eq. (3.19). In the result (5.1), the sum over s is a sum over the relevant species (flavors) of quarks (i.e., u, d, s, c, ...), and the current matrix elements are given by the fermionic case of eq. (3.36). $N_s = 4$ counts the spin and particle/anti-particle states for each flavor of quark, and $d_R = 3$ is the number of colors of a quark. As usual, $n_{\rm f}(\omega) = 1/(e^{\beta\omega}+1)$ is the Fermi distribution function. In the result (5.1), the contribution to the $p_\parallel$ integral from $p_\parallel > 0$ corresponds to bremsstrahlung from quarks, the $p_\parallel < -k$ contribution is identical (after substituting $p_\parallel \to -k - p_\parallel$) and accounts for bremsstrahlung from anti-quarks, and the $-k < p_\parallel < 0$ contribution corresponds to pair annihilation.

All dependence on the nature of the scatterers which influence the photon emission rate is contained in the relevant $\langle\!\langle AA \rangle\!\rangle$ correlator. As discussed earlier [*c.f.* eq. (2.4)], the background field correlator is given by $2[n_{\rm b}(q^0)+1]\,{\rm Im}\,G_{\rm Ret}(Q)$, with the gluon propagator evaluated in the hard thermal loop approximation for soft momenta $Q \ll T$. Using standard results for the hard thermal loop self-energy, one finds the gauge-invariant[21] correlation [25]

$$\left\langle\!\!\left\langle A^-(Q)\,[A^-(Q)]^* \right\rangle\!\!\right\rangle_{q^0=q_\parallel} = \frac{\pi m_{\rm D}^2 T}{2q} \left\{ \frac{2}{|q^2 - \Pi_{\rm L}(Q)|^2} + \frac{(q_\perp/q)^4}{|q^2 - (q^0)^2 + \Pi_{\rm T}(Q)|^2} \right\}_{q^0=q_\parallel}, \tag{5.3}$$

when q^0 is set equal to $q_\parallel$ by the delta-function in eq. (5.2). Here, $m_{\rm D}$ is the (lowest-order) color Debye mass, given by $m_D^2 = (1 + \frac{1}{6}N_{\rm f})\,g^2 T^2$ for QCD with $N_{\rm f}$ flavors, and[22]

$$\Pi_{\rm L}(Q) = m_{\rm D}^2 \left[-1 + \frac{q^0}{2q} \ln\frac{q+q^0}{q-q^0} - i\,\frac{\pi q^0}{2q} \right], \tag{5.4}$$

$$\Pi_{\rm T}(Q) = m_{\rm D}^2\,\frac{[q^2-(q^0)^2]}{2q^2} \left[\frac{(q^0)^2}{q^2-(q^0)^2} + \frac{q^0}{2q} \ln\frac{q+q^0}{q-q^0} - i\,\frac{\pi q^0}{2q} \right]. \tag{5.5}$$

Together with eqs. (5.1) and (5.2), this reproduces our previous results of ref. [25].

6. Gluon emission

We now wish to extend of the above analysis to the case of gluon emission. Other authors who have considered the LPM effect have also discussed gluon emission [20]–[24]. Our generalization is similar to these previous treatments, but our final result is the first to

[21] The change in the $\langle A^-(Q) A^-(Q)^* \rangle$ correlator under an abelian gauge transformation is proportional to $q^- \equiv q^0 - q_\parallel$, but we are evaluating at $q^- = 0$. Hence this change vanishes for any transformation whose Fourier transform is non-singular at $q^- = 0$ (e.g., any transformation of compact support). Because gauge field fluctuations on the gT scale are perturbative, the non-abelian part of a gauge transformation changes the correlator by a subleading amount suppressed by g.

[22] In the convention used here, the hard thermal loop self-energy $\Pi^{\mu\nu}(Q) = (Q^2/q^2)\,\Pi_{\rm L}(Q)\,\mathcal{P}_{\rm L}^{\mu\nu} + \Pi_{\rm T}(Q)\,\mathcal{P}_{\rm T}^{\mu\nu}$, where $\mathcal{P}_{\rm L}$ and $\mathcal{P}_{\rm T}$ are longitudinal and transverse projection operators. Various other authors (sometimes including ourselves) instead use the notation $\Pi_{\rm L}(Q)$ to denote our $-(Q^2/q^2)\,\Pi_{\rm L}(Q)$.

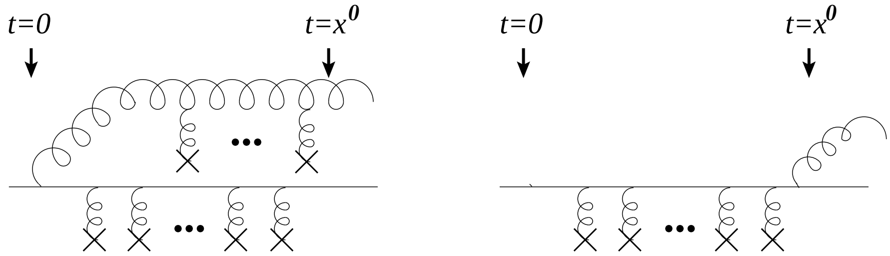

Figure 17: Two diagrams, time ordered from left to right, whose interference contributes to the rate of gluon bremsstrahlung. The only difference from the photon emission case of figure 7 is that the gluon, as well as the emitter, can interact with the soft background field.

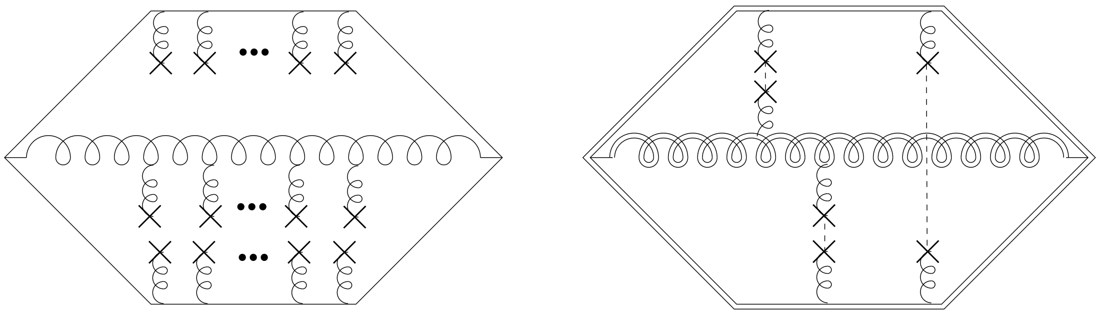

Figure 18: A single diagram depicting the interference of the two gluon emission amplitudes of figure 17. The left-hand version depicts the product of amplitudes in a given background field; the right-hand version shows the result after averaging over random background fields. Individual background field correlators can connect any two of the three hard lines, and double lines represent the resummed propagators of figure 14.

give the full correct leading-order answer at high temperature because it is the first to treat correctly the dynamics of the scatterers.

The key difference from photons is that the gluon also carries color. So, whereas the photon merely contributed a phase $\exp(ik^0 t)$ to the time evolution amplitude, an emitted hard gluon will feel the random colored background field, just as the emitting particle does. But provided we consider *hard* gluon emission, the emitted gluon is distinct from the soft background, and should be treated as another (quasi)particle. The analog of figure 7 for gluon emission is shown in figure 17. The analogs of figure 9 and figure 13 are shown in figure 18. Much of the argument for photon emission still holds; the gluon and quark must be nearly collinear, and consequently the interactions are ordered in the same way as before. The new complications are, first, that there is a color matrix T^A_{ab} at the hard particle vertex, and second, that there are now correlations between the soft gauge field felt by the gluon and either emitter line, not just between the two emitter lines.

Because the interactions are ordered as before, it is still possible to resum the diagrams by an integral equation similar to eq. (3.14). The only difference is that there are now three elements in the collision term, corresponding to the three kinds of correlations between lines shown in figure 18. The group theoretic coefficients are easily found with the help of

$$T_R^b\, T_R^a\, T_R^b = \left(C_R - \frac{1}{2} C_{\rm A}\right) T_R^a\,, \qquad T_R^c\, T_R^b\, i f^{abc} = \frac{1}{2}\, C_{\rm A}\, T_R^a\,, \tag{6.1}$$

where T_R^a denote representation R color generators. Since the soft gluon correlators are ordered in time, this is sufficient to determine the group factor for the whole diagram; each line between emitters gives a factor of $(C_R - \frac{1}{2}C_{\rm A})$ and each line from an emitter to the emitted gluon gives $\frac{1}{2}C_{\rm A}$.

The other complication is that, whereas before a cross-rung always changed $\mathbf{p}$ and left $\mathbf{k}$ the same, now it can either change $\mathbf{p}$, change $\mathbf{k}$, or change both. This is a reflection of the fact that the gluon, unlike the photon, can scatter during the $1/g^2T$ time scale of the process. In the photon case, we had a natural fixed direction $\mathbf{k}$ with respect to which we defined $\mathbf{p}_\perp$ (whose changes we had to keep track of) and $p_\parallel$ (whose changes we could ignore).

One inelegant but concrete possibility for the gluon case would be to proceed as before but (i) pick by some convention any direction nearly collinear with $\mathbf{k}$, $\mathbf{p}$ and $\mathbf{p}+\mathbf{k}$ to define the "parallel" ($\|$) direction, and (ii) keep track of changes to $\mathbf{k}_\perp$ as well as $\mathbf{p}_\perp$. For example, consider picking the $\|$ direction to be that of the momentum of the emitted gluon line at the right-most corner of figure 18. The analog to our results for photon emission would then be[23]

$$\begin{aligned} \frac{d\Gamma_{\rm g}^{\rm LPM}}{d^3\mathbf{k}} &= \frac{d\Gamma_{\rm g}^{\rm LPM}}{4\pi k^2\, dk} \\ &= \frac{\alpha_{\rm s}}{4\pi^2 k} \sum_s N_s\, d_s\, C_s \int_{-\infty}^{+\infty} \frac{dp_\parallel}{2\pi} \left\{ \int \frac{d^2\mathbf{p}_\perp}{(2\pi)^2}\, \frac{d^2\mathbf{k}_\perp}{(2\pi)^2}\, n_s(p_\parallel{+}k_\parallel)\, [1 \mp n_s(p_\parallel)]\, [1 + n_b(k_\parallel)] \right. \\ &\qquad \left. \times\, |\mathcal{J}^{(s)}_{p_\parallel \leftarrow p_\parallel + k_\parallel}|^2\; 2\boldsymbol{\Delta}_{\mathbf{pk}} \cdot {\rm Re}\, \mathbf{f}_s(\mathbf{p}_\perp, \mathbf{k}_\perp; p_\parallel, k_\parallel) \right\} \Bigg|_{k_\parallel \to k}, \end{aligned} \tag{6.2}$$

where we have included a radiation stimulation factor $1{+}n_b(k)$, and defined $\boldsymbol{\Delta}_{\mathbf{pk}} \equiv \mathbf{p}_\perp - p_\parallel \mathbf{k}_\perp / k_\parallel$ as the component of $\mathbf{p}$ perpendicular to $\mathbf{k}$ (at leading order). For hard gluon emission, the soft $O(gT)$ changes to $\mathbf{k}$ during the formation time are small compared to $\mathbf{k}$ itself. This is why we can define the differential hard gluon emission rate $d\Gamma_{\rm g}/d^3k$ at leading order even though, due to soft collisions, the momentum $\mathbf{k}$ of the emitted hard gluon is only an approximate concept (as is manifest by the integral over soft $\mathbf{k}_\perp$ on the

[23] $d\Gamma_{\rm g}^{\rm LPM}/d^3k$ represents the differential rate per unit volume of processes that increase by one the number of gluons with momentum $\mathbf{k}$. Rotation invariance implies it is only a function of the magnitude $k = |\mathbf{k}|$ (which is all that the right-hand-side depends on after the indicated identification $k_\parallel \to k$). One might be tempted to think that the integral of this quantity is the rate per unit volume of processes that increase the total gluon number by one. This is incorrect since pair annihilation of hard gluons contributes to $d\Gamma_{\rm g}^{\rm LPM}/d^3k$ but decreases rather than increases the total number of gluons. In addition, once one integrates over $\mathbf{k}$, one has to avoid double counting final states in the bremsstrahlung process. We are unaware of any simple physical interpretation of the integral of our $d\Gamma_{\rm g}^{\rm LPM}/d^3k$, although this differential rate is closely related to ingredients needed in the evaluation of various physical quantities, such as leading-order transport coefficients [17].

JHEP06(2002)030

right-hand side above). The sum over species in (6.2) now includes both gluons and quarks and we have introduced d_s and C_s as the color representation dimension and quadratic Casimir for species s (so $d_s = d_{\rm F} = 3$ and $C_s = C_{\rm F} = 4/3$ for quarks, while $d_s = d_{\rm A} = 8$ and $C_s = C_{\rm A} = 3$ for gluons). Once again, N_s denotes the number of spin states (including anti-particles) for the species, so $N_s = 4$ for quarks and $N_s = 2$ for gluons. The accompanying integral equation is

$$
\begin{aligned}
2\boldsymbol{\Delta}_{\mathbf{pk}}\,(2\pi)^2\,\delta^{(2)}(\mathbf{k}_\perp) = {}& i\,\delta E\,\mathbf{f}_s(\mathbf{p}_\perp,\mathbf{k}_\perp;p_\parallel,k_\parallel) + g^2\int_Q 2\pi\,\delta(q^0{-}q_\parallel)\,\left\langle\!\!\left\langle A^-(Q)\,[A^-(Q)]^*\right\rangle\!\!\right\rangle \times \\
& \times\Big\{\Big(C_s-\frac{1}{2}C_{\rm A}\Big)\left[\mathbf{f}_s(\mathbf{p}_\perp,\mathbf{k}_\perp;p_\parallel,k_\parallel)-\mathbf{f}_s(\mathbf{p}_\perp{-}\mathbf{q}_\perp,\mathbf{k}_\perp;p_\parallel,k_\parallel)\right]+ \\
& +\frac{1}{2}C_{\rm A}\left[\mathbf{f}_s(\mathbf{p}_\perp,\mathbf{k}_\perp;p_\parallel,k_\parallel)-\mathbf{f}_s(\mathbf{p}_\perp{+}\mathbf{q}_\perp,\mathbf{k}_\perp{-}\mathbf{q}_\perp;p_\parallel,k_\parallel)\right]+ \\
& +\frac{1}{2}C_{\rm A}\left[\mathbf{f}_s(\mathbf{p}_\perp,\mathbf{k}_\perp;p_\parallel,k_\parallel)-\mathbf{f}_s(\mathbf{p}_\perp,\mathbf{k}_\perp{+}\mathbf{q}_\perp;p_\parallel,k_\parallel)\right]\Big\}. \qquad (6.3)
\end{aligned}
$$

The three terms in the integral correspond respectively to gluon exchange between the top and bottom rails, the top and middle rails, and the bottom and middle rails of figure 18. The momenta flowing from left to right in the top, middle, and bottom rails of that figure have been labeled $\mathbf{p}$, $\mathbf{k}$, and $-\mathbf{p}-\mathbf{k}$, respectively. The energy difference δE (for which we have suppressed the arguments $\mathbf{p}_\perp, \mathbf{k}_\perp, p_\parallel$ and $k_\parallel$) is

$$
\delta E \equiv \frac{m_{\rm g}^2+k_\perp^2}{2k_\parallel}+\frac{m_s^2+p_\perp^2}{2p_\parallel}+\frac{m_s^2+|\mathbf{p}_\perp{+}\mathbf{k}_\perp|^2}{2(-p_\parallel{-}k_\parallel)} \simeq E_{\rm g}+E_{\mathbf{p}}-E_{\mathbf{p+k}}\,. \qquad (6.4)
$$

This expression incorporates the fact that in an equilibrated thermal plasma, the hard gluon dispersion relation includes an effective mass $m_{\rm g}^2 = m_{\rm D}^2/2$.

The thermal widths associated with the three rails generate forward-scattering contributions in the integral equation (6.3) equal to $(\Gamma_{\rm g}{+}\Gamma_{\mathbf{p}}{+}\Gamma_{\mathbf{p+k}})\,\mathbf{f}_s(\mathbf{p}_\perp,\mathbf{k}_\perp;p_\parallel,k_\parallel)$. Each width has the form given in eq. (3.28) but containing the appropriate quadratic Casimir (C_s or $C_{\rm A}$), so that $\Gamma_{\rm g}{+}\Gamma_{\mathbf{p}}{+}\Gamma_{\mathbf{p+k}} \simeq g^2\,(2C_s+C_{\rm A})\int_Q \pi\delta(q^0{-}q_\parallel)\,\left\langle\!\!\left\langle A^-(Q)\,[A^-(Q)]^*\right\rangle\!\!\right\rangle$. These forward-scattering contributions have been suitably combined with the three different collision terms to form the manifestly infrared-safe differences appearing in the integral equation (6.3).

The preceding is a valid but inelegant approach because it does not exploit the rotational invariance of the problem. Other than $|\mathbf{f}_s|$, the elements of the integrand in the rate formula (6.2) are invariant under small angle ($\theta \sim g$) rotations, which do not change $p_\parallel$ and $k_\parallel$ at leading order, but do change $\mathbf{p}_\perp$ and $\mathbf{k}_\perp$. So one could split the $d^2p_\perp\,d^2k_\perp$ into one integral with respect to the relative momentum $\Delta_{\mathbf{pq}}$, which appears explicitly in (6.2), and another integral over small rotations. The integration over small rotations could then be absorbed into $\mathbf{f}_{\rm s}$, defining a new function that depends only on $\Delta_{\mathbf{pq}}$. It turns out that the most symmetric procedure does not use $\Delta_{\mathbf{pq}}$ but rather the quantity $\mathbf{h} \equiv k_\parallel \Delta_{\mathbf{pq}}$, which can be written as

$$
\mathbf{h} = k_\parallel\,\mathbf{p}_\perp - p_\parallel\,\mathbf{k}_\perp\,. \qquad (6.5)
$$

This may also be written as $\mathbf{h} = (\mathbf{k}\times\mathbf{p})\times\mathbf{e}_{\|}$, where $\mathbf{e}_{\|}$ is the unit vector in the $\|$ direction. The corresponding equations that only track changes in $\mathbf{h}$ are

$$\frac{d\Gamma_{\rm g}^{\rm LPM}}{d^3\mathbf{k}} = \frac{\alpha_{\rm s}}{4\pi^2 k^2} \sum_s N_s\, d_s\, C_s \int_{-\infty}^{+\infty} \frac{dp}{2\pi} \int \frac{d^2\mathbf{h}}{(2\pi)^2}\, n_s(p{+}k)\, [1 \mp n_s(p)]\, [1 + n_b(k)] \\ \times \frac{1}{k^3}\, |\mathcal{J}^{(s)}_{p\leftarrow p+k}|^2\; 2\mathbf{h}\cdot {\rm Re}\,\mathbf{F}_s(\mathbf{h};p,k)\,, \qquad (6.6)$$

where $\mathbf{F}_s(\mathbf{h};p,k)$ is the solution to the integral equation

$$2\mathbf{h} = i\,\delta E(h;p,k)\,\mathbf{F}_s(\mathbf{h};p,k) + g^2 \int_Q 2\pi\,\delta(q^0{-}q_{\|})\, \Big\langle\!\Big\langle A^-(Q)\,[A^-(Q)]^* \Big\rangle\!\Big\rangle \times \qquad (6.7) \\ \times \bigg\{ \Big(C_s - \frac{1}{2}C_{\rm A}\Big)\, [\mathbf{F}_s(\mathbf{h};p,k) - \mathbf{F}_s(\mathbf{h}{-}k\,\mathbf{q}_\perp;p,k)] + \\ + \frac{1}{2}C_{\rm A}\, [\mathbf{F}_s(\mathbf{h};p,k) - \mathbf{F}_s(\mathbf{h}{+}(k{+}p)\mathbf{q}_\perp;p,k)] + \\ + \frac{1}{2}C_{\rm A}\, [\mathbf{F}_s(\mathbf{h};p,k) - \mathbf{F}_s(\mathbf{h}{-}p\,\mathbf{q}_\perp;p,k)] \bigg\},$$

with

$$\delta E(h;p,k) = \frac{m_{\rm g}^2}{2k} + \frac{m_s^2}{2p} + \frac{m_s^2}{2(-p-k)} - \frac{h^2}{2p\,k\,(-p-k)}\,. \qquad (6.8)$$

To simplify the appearance of these results, and the equations below, we have dropped the $\|$ subscripts on $p_{\|}$ and $k_{\|}$. It should be emphasized that evaluating these expressions does not, in fact, require selecting any particular convention for defining the $\|$ direction. Also, note that rotation invariance implies that $\mathbf{F}_s(\mathbf{h};p,k)$ must equal $\mathbf{h}$ times a scalar function of $|\mathbf{h}|$, $p_{\|}$, and k, but the integral equation (6.7) is more compact if $\mathbf{F}_s(\mathbf{h};p,k)$ is left as a vector function.

The splitting function for gluons is

$$P_{gg\leftarrow g}(z) = \frac{1+z^4+(1{-}z)^4}{z\,(1{-}z)} \qquad (6.9)$$

for $z<1$, so that

$$|\mathcal{J}^{(g)}_{p\leftarrow p+k}|^2 = \frac{p^4+k^4+(p{+}k)^4}{8p^3\,(p{+}k)^3}\,. \qquad (6.10)$$

This expression, when multiplied by k^{-3}, is symmetric under interchanges of the three gluon momenta p, k, and $-p{-}k$.

Further symmetry of our result (whether for quark or gluon emitters) can be made manifest by rewriting group factors so that the expression in curly braces in the integral equation (6.7) is

$$\bigg\{ \frac{1}{2}(C_{R_3}+C_{R_1}-C_{R_2})\,[\mathbf{F}_s(\mathbf{h};p,k) - \mathbf{F}_s(\mathbf{h}{-}p_2\,\mathbf{q}_\perp;p,k)] + \\ + \frac{1}{2}(C_{R_1}+C_{R_2}-C_{R_3})\,[\mathbf{F}_s(\mathbf{h};p,k) - \mathbf{F}_s(\mathbf{h}{-}p_3\,\mathbf{q}_\perp;p,k)] + \\ + \frac{1}{2}(C_{R_2}+C_{R_3}-C_{R_1})\,[\mathbf{F}_s(\mathbf{h};p,k) - \mathbf{F}_s(\mathbf{h}{-}p_1\,\mathbf{q}_\perp;p,k)] \bigg\}, \qquad (6.11)$$

where (p_1, p_2, p_3) denotes the three momenta $(p, k, -p-k)$ and $(C_{R_1}, C_{R_2}, C_{R_3})$ denote the quadratic Casimirs $(C_s, C_{\mathrm{A}}, C_s)$ of the corresponding color representations.[24]

The previous photon emission result can be extracted from the final gluon emission expressions (6.6)–(6.8) by setting $C_{\mathrm{A}}=0$ inside the integral equation (which corresponds to making the emitted particle colorless rather than in the adjoint representation), replacing C_s in eq. (6.6) with q_s^2, and using the photon, rather than gluon, thermal mass in the expression (6.8) for δE. (The resulting photon thermal mass contribution to δE is irrelevant for hard photons [25].)

Finally, we make a last note about the cancellation of infrared divergences in our result for gluon production. The fact that the collision term in (6.7) only involves differences of the form $\mathbf{F}_s(\mathbf{h}; p, k) - \mathbf{F}_s(\mathbf{h} - p_i \mathbf{q}_\perp; p, k)$, which cancel in the far-infrared ($\mathbf{q}_\perp \to 0$) limit, results from including all three ways of connecting the three rails in figure 18 together with resumming self-energies (as in figure 14) on all three rails. In contrast, if we had truncated the hard gluon line and evaluated the earlier diagrams of figure 13 with external color currents, these cancellations would have been absent and our result would have had far-infrared divergences signalling sensitivity to ultra-soft momentum scales. The sensitivity of such truncated diagrams to ultra-soft physics is relevant to the evaluation of quantities such as color conductivity,[25] but not to the problem of the hard gluon emission rate at leading order.

Acknowledgments

This work was supported, in part, by the U.S. Department of Energy under Grant Nos. DE-FG03-96ER40956 and DE-FG02-97ER41027. We thank Francois Gelis and Patrick Aurenche for helpful conservations.

References

[1] E.V. Shuryak, *Quark-gluon plasma and hadronic production of leptons, photons and psions*, *Phys. Lett.* **B 78** (1978) 150, [*Sov. J. Nucl. Phys.* **28** (1978) 408, *Yad. Fiz.* **28** (1978) 796].

[2] K. Kajantie and H.I. Miettinen, *Temperature measurement of quark-gluon plasma formed in high-energy nucleus-nucleus collisions*, *Z. Physik* **C 9** (1981) 341.

[3] K. Kajantie and P.V. Ruuskanen, *Shielding of quark mass singularities in photon emission from hot quark-gluon plasma*, *Phys. Lett.* **B 121** (1983) 352.

[24] There is a general argument that gives the structure of the group factors shown in eq. (6.11) even if R_1, R_2, and R_3 were any three color representations. Color conservation at either end of figure 18 means that these three representations have to be combined into a color singlet. Acting on that color singlet state with color generators $T^a_{R_1} + T^a_{R_2} + T^a_{R_3}$ should give zero. So acting with $T^a_{R_1} + T^a_{R_2}$ has the same effect as acting with $-T^a_{R_3}$. Squaring both sides and summing over the basis a of the algebra, one then obtains that $T^a_1 T^a_2$ (the factor associated with exchanging a gluon between particles 1 and 2), acting on the color singlet, is equivalent to multiplication by $\frac{1}{2}(C_3 - C_1 - C_2)$. The other group factors in (6.11) follow by permutation.

[25] For a discussion of color conductivity in terms of ladder diagrams, see ref. [38]. For an equivalent discussion in terms of kinetic theory, see ref. [39] and the pathbreaking work of ref. [40]. See also refs. [41, 42] and the original, early work of ref. [43].

[4] F. Halzen and H.C. Liu, *Experimental signatures of phase transition to quark matter in high-energy collisions of nuclei*, *Phys. Rev.* **D 25** (1982) 1842.

[5] B. Sinha, *Universal signals of quark-gluon plasma*, *Phys. Lett.* **B 128** (1983) 91.

[6] R.C. Hwa and K. Kajantie, *Diagnosing quark matter by measuring the total entropy and the photon or dilepton emission rates*, *Phys. Rev.* **D 32** (1985) 1109.

[7] G. Staadt, W. Greiner and J. Rafelski, *Photons from strange quark annihilation in quark-gluon plasma*, *Phys. Rev.* **D 33** (1986) 66.

[8] M. Neubert, *Photon production in ultrarelativistic heavy ion collisions at 200-Gev/U*, *Z. Physik* **C 42** (1989) 231.

[9] J. Kapusta, P. Lichard and D. Seibert, *High-energy photons from quark-gluon plasma versus hot hadronic gas*, *Phys. Rev.* **D 44** (2774) 1991. Erratum: *Phys. Rev.* **D 47** (4171) 1991.

[10] R. Baier, H. Nakkagawa, A. Niegawa and K. Redlich, *Production rate of hard thermal photons and screening of quark mass singularity*, *Z. Physik* **C 53** (1992) 433.

[11] P. Aurenche, F. Gelis, R. Kobes and H. Zaraket, *Bremsstrahlung and photon production in thermal QCD*, *Phys. Rev.* **D 58** (1998) 085003 [hep-ph/9804224].

[12] P. Aurenche, F. Gelis and H. Zaraket, *KLN theorem, magnetic mass and thermal photon production*, *Phys. Rev.* **D 61** (2000) 116001 [hep-ph/9911367].

[13] P. Aurenche, F. Gelis and H. Zaraket, *Landau-Pomeranchuk-Migdal effect in thermal field theory*, *Phys. Rev.* **D 62** (2000) 096012 [hep-ph/0003326].

[14] F.D. Steffen and M.H. Thoma, *Hard thermal photon production in relativistic heavy ion collisions*, *Phys. Lett.* **B 510** (2001) 98 [hep-ph/0103044].

[15] T. Peitzmann and M.H. Thoma, *Direct photons from relativistic heavy-ion collisions*, *Phys. Rept.* **364** (2002) 175 [hep-ph/0111114].

[16] T. Peitzmann, *Direct photon production in heavy ion reactions at SPS and RHIC*, nucl-ex/0201003.

[17] P. Arnold, G. D. Moore, and L. G. Yaffe, *Transport coefficients in high temperature gauge theories: beyond leading log*, in preparation.

[18] B.G. Zakharov, *Fully quantum treatment of the Landau-Pomeranchuk-Migdal effect in QED and QCD*, *Sov. Phys. JETP Lett.* **63** (1996) 952 [hep-ph/9607440]; *Radiative energy loss of high energy quarks in finite-size nuclear matter and quark-gluon plasma*, *Sov. Phys. JETP Lett.* **65** (1997) 615 [hep-ph/9704255]; *Light-cone path integral approach to the Landau-Pomeranchuk-Migdal effect*, *Phys. Atom. Nucl.* **61** (1998) 838 [hep-ph/9807540].

[19] R. Baier, Y.L. Dokshitzer, A.H. Mueller and D. Schiff, *Medium-induced radiative energy loss: equivalence between the BDMPS and Zakharov formalisms*, *Nucl. Phys.* **B 531** (1998) 403 [hep-ph/9804212].

[20] R. Baier, D. Schiff and B.G. Zakharov, *Energy loss in perturbative QCD*, *Ann. Rev. Nucl. Part. Sci.* **50** (2000) 37 [hep-ph/0002198].

[21] B.G. Zakharov, *Quark energy loss in an expanding quark-gluon plasma*, hep-ph/9807396; *On the energy loss of high energy quarks in a finite-size quark gluon plasma*, *Sov. Phys. JETP Lett.* **73** (2001) 49 [hep-ph/0012360].

JHEP06(2002)030

[22] R. Baier, Y.L. Dokshitzer, S. Peigne and D. Schiff, *Induced gluon radiation in a QCD medium*, *Phys. Lett.* **B 345** (1995) 277 [hep-ph/9411409];
R. Baier, Y.L. Dokshitzer, A.H. Mueller and D. Schiff, *Angular dependence of the radiative gluon spectrum and the energy loss of hard jets in QCD media*, *Phys. Rev.* **D 60** (1999) 064902 [hep-ph/9907267].

[23] R. Baier, Y.L. Dokshitzer, A.H. Mueller, S. Peigne and D. Schiff, *Radiative energy loss of high energy quarks and gluons in a finite-volume quark-gluon plasma*, *Nucl. Phys.* **B 483** (1997) 291 [hep-ph/9607355];
R. Baier, Y.L. Dokshitzer, A.H. Mueller, S. Peigne and D. Schiff, *Radiative energy loss and p(t)-broadening of high energy partons in nuclei*, *Nucl. Phys.* **B 484** (1997) 265 [hep-ph/9608322].

[24] M. Gyulassy and X.-n. Wang, *Multiple collisions and induced gluon bremsstrahlung in QCD*, *Nucl. Phys.* **B 420** (1994) 583 [nucl-th/9306003].

[25] P. Arnold, G.D. Moore and L.G. Yaffe, *Photon emission from ultrarelativistic plasmas*, *J. High Energy Phys.* **11** (2001) 057 [hep-ph/0109064].

[26] P. Arnold, G.D. Moore and L.G. Yaffe, *Photon emission from quark gluon plasma: complete leading order results*, *J. High Energy Phys.* **12** (2001) 009 [hep-ph/0111107].

[27] E. Wang and U. Heinz, *A generalized fluctuation-dissipation theorem for nonlinear response functions*, hep-th/9809016.

[28] L.D. Landau and I. Pomeranchuk, *Limits of applicability of the theory of bremsstrahlung electrons and pair production at high-energies*, *Dokl. Akad. Nauk Ser. Fiz.* **92** (1953) 535; *Electron cascade process at very high-energies*, *Dokl. Akad. Nauk Ser. Fiz.* **92** (1953) 735. These two papers are also available in English in L. Landau, *The collected papers of L.D. Landau* Pergamon Press, New York, 1965.

[29] A. B. Migdal, *Dokl. Akad. Nauk Ser. Fiz.* **105** (1955) 77.

[30] A.B. Migdal, *Bremsstrahlung and pair production in condensed media at high-energies*, *Phys. Rev.* **103** (1956) 1811.

[31] R. Blankenbecler and S. D. Drell, *The Landau-Pomeranchuk-Migdal effect for finite targets*, *Phys. Rev.* **D 53** (1996) 6265.

[32] R. Baier, Y.L. Dokshitzer, A.H. Mueller, S. Peigne and D. Schiff, *The Landau-Pomeranchuk-Migdal effect in QED*, *Nucl. Phys.* **B 478** (1996) 577 [hep-ph/9604327].

[33] B.G. Zakharov, *Landau-Pomeranchuk-Migdal effect for finite-size targets*, *Pisma Zh. Eksp. Teor. Fiz.* **64** (1996) 737 [hep-ph/9612431]; *Light-cone path integral approach to the Landau-Pomeranchuk-Migdal effect and SLAC data on bremsstrahlung from high-energy electrons*, *Phys. Atom. Nucl.* **62** (1999) 1008 [hep-ph/9805271].

[34] S. Klein, *Suppression of bremsstrahlung and pair production due to environmental factors*, *Rev. Mod. Phys.* **71** (1999) 1501 [hep-ph/9802442].

[35] V.V. Klimov, *Spectrum of elementary Fermi excitations in quark gluon plasma*, *Sov. J. Nucl. Phys.* **33** (1981) 934 [*Yad. Fiz.* **33** (1981) 1734].

[36] H.A. Weldon, *Effective fermion masses of order gT in high temperature gauge theories with exact chiral invariance*, *Phys. Rev.* **D 26** (1982) 2789.

[37] R.D. Pisarski, *Damping rates for moving particles in hot QCD*, *Phys. Rev.* **D 47** (1993) 5589.

[38] J.M. Martinez Resco and M.A. Valle Basagoiti, *Color conductivity and ladder summation in hot QCD*, *Phys. Rev.* **D 63** (2001) 056008 [hep-ph/0009331].

[39] P. Arnold, D.T. Son and L.G. Yaffe, *Hot B violation, color conductivity and* $\log(1/\alpha)$ *effects*, *Phys. Rev.* **D 59** (1999) 105020 [hep-ph/9810216].

[40] D. Bödeker, *On the effective dynamics of soft non-abelian gauge fields at finite temperature*, *Phys. Lett.* **B 426** (1998) 351 [hep-ph/9801430]; *From hard thermal loops to Langevin dynamics*, *Nucl. Phys.* **B 559** (1999) 502 [hep-ph/9905239].

[41] D.F. Litim and C. Manuel, *Mean field dynamics in non-abelian plasmas from classical transport theory*, *Phys. Rev. Lett.* **82** (1999) 4981 [hep-ph/9902430].

[42] J.-P. Blaizot and E. Iancu, *A Boltzmann equation for the QCD plasma*, *Nucl. Phys.* **B 557** (1999) 183 [hep-ph/9903389].

[43] A. Selikhov and M. Gyulassy, *Color diffusion and conductivity in a quark-gluon plasma*, *Phys. Lett.* **B 316** (1993) 373 [nucl-th/9307007].